Table 3 Frequency of the lactoferrin genotype in healthy volunteers

	Lactoferrin Glu561Asp	Number of subjects	Frequency of genotype (%)
No polymorphism	−/−	31	56.3
Heterozygote	+/−	18	32.7
Homozygote	+/+	7	12.7

determine the frequency of the lactoferrin Glu561Asp gene in 56 healthy Japanese volunteers. Comparison of this frequency in healthy volunteers with the frequency in patients revealed significant polymorphism in the patients (Fisher's exact test = 0.0119, $p<0.01$)(table 3).

DISCUSSION

We suggested in this study that lactoferrin Glu561Asp facilitates amyloid formation in corneal amyloidosis with trichiasis. We speculate that lactoferrin from tears should be a source of amyloid formation in the cornea of patients for the following four reasons. Firstly, lactoferrin is the major component of tears. Secondly, anti-human lactoferrin antibody reactive mass stuck to cilia (fig 2D). Thirdly, lactoferrin was clearly detected in the intracellular space of the corneal epithelium. And fourthly, lactoferrin was observed in amyloid deposits in all samples examined (fig 2). Although we cannot deny the possibility that continuous stimulation by trichiasis may induce corneal epithelial cells and stromal fibroblasts to secrete the amyloidogenic protein, because these cells have the potential producing amyloid protein in certain situations,[22] we conclude that mutated lactoferrin derived from tears might infiltrate into the site of amyloid deposition through the extracellular space of the epithelial cells. We also performed the lactoferrin gene analysis and histochemistry of three samples of corneal amyloidosis with keratoconus. Although anti-lactoferrin antibody showed a positive reaction, no polymorphism in the lactoferrin gene was detected (data not shown). In this type of amyloidosis, the parenchyma already has abnormal structures that may show an affinity with native lactoferrin. But, in corneal amyloidosis with trichiasis, the polymorphism may be an indispensable factor because the parenchyma, the targeted lesion of amyloid deposition, has normal structures.

We carefully checked the pattern of anti-lactoferrin antibody reactivity of lactoferrin Glu561Asp gene in the heterozygotic and homogygotic patients. However, no obvious difference was detected. This may be because the degree of the amyloidotic changes in the corneal may be too immature to be compared. Accumulation of such cases for comparison is needed.

We previously reported that lactoferrin forms an amyloid mass both in in vitro examination and in the cornea.[16] However, the relation between lactoferrin gene polymorphisms and the amyloid formation mechanism remained to be elucidated because statistical differences in the frequency of the polymorphism between the patients and control subjects was not clear.

To investigate whether the mutated form of lactoferrin has amyloidogenic ability, a possible conformational change of the protein was simulated. According to the PDB code (www.rcsb.org/), the amino acid at position 561 in lactoferrin locates in a loop region at the bottom of the C-lobe (fig 4A). This loop region has relatively high B factors, which indicates this region's flexibility.[23] Oxygen of the Glu561 side chain forms a weak hydrogen bond with the side chain's nitrogen atom of Trp563 at a distance of 3.32 Å (fig 4B). The polymorphism of Glu561Asp in lactoferrin seems to have no hydrogen bond or has a weaker interaction with Trp563. This might enhance flexibility of this loop region, and then

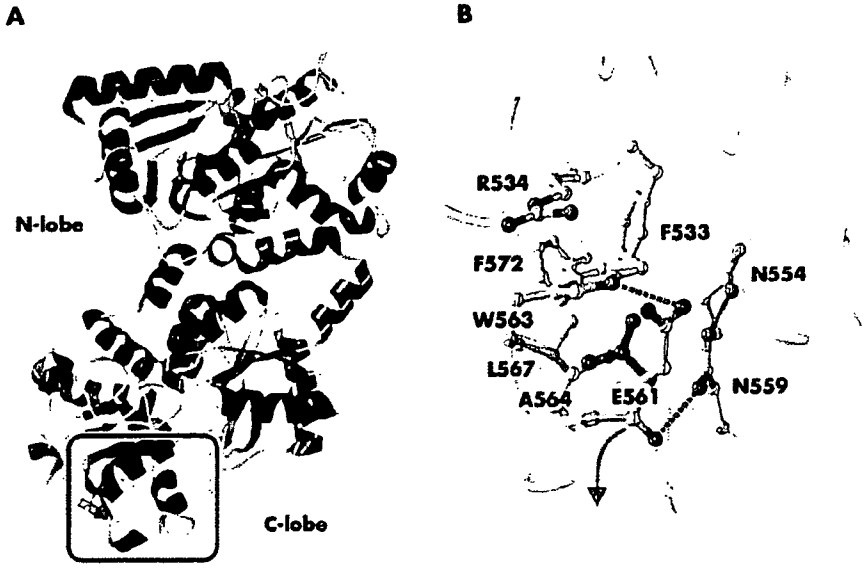

Figure 4 Structural feature of the human lactoferrin Glu561. (A) A ribbon diagram of human lactoferrin. The region depicted in close up (B) is indicated by a rectangle. (B) The main chain backbone is shown in grey. The residues, which involve the charged or hydrophobic interaction network in this region, are shown as a ball and stick model. The Asp mutated from Glu561 is shown in purple.

expose the hydrophobic patch. Consequently, the mutant lactoferrin may form amyloid fibrils via this exposed hydrophobic patch.

Clinically, our nine patients showed the two different types of amyloidosis. It is well known that hereditary corneal amyloidosis has been classified into two types, gelatinous and lattice,[24] with a pathogenesis related to mutated M1S1[25 26] and TGFBI[27] genes, respectively. Majima *et al* speculated that amyloid deposition in the corneal stroma resulted in a lattice pattern and deposition in the epithelium resulted in a gelatinous pattern (personal communication). From our patients' clinical observations, we derive the following: in gelatinous-type secondary corneal amyloidosis, lactoferrin aggregates into the epithelial layer through the extracellular space of the epithelium where cilia repeatedly touch. In contrast, in lattice-type secondary corneal amyloidosis, epithelial erosion with destruction of Bowman's membrane might enable lactoferrin to integrate into the stroma and form amyloid deposition.

From our study, we conclude that secondary corneal amyloidosis with trichiasis is predominantly induced by both trichiasis and lactoferrin Glu561Asp polymorphism.

ACKNOWLEDGEMENTS

This work was supported by grants from the Amyloidosis Research Committee, the Pathogenesis, Therapy of Hereditary Neuropathy Research Committee, the Surveys and Research on Specific Disease, the Ministry of Health and Welfare of Japan, Charitable Trust Clinical Pathology Research Foundation of Japan, and Research for the Future Program Grant, and Grants in Aid for Scientific Research (B) 15390275 and (B) 20253742 from the Ministry of Education, Science, Sports and Culture of Japan. The authors thank Hiroko Katsura, and Miyo Okajima for technical assistance.

Authors' affiliations

K Araki-Sasaki, T Kawaji, K Matsumoto, H Tanihara, Department of Ophthalmology, Graduate School of Medical Sciences, Kumamoto University, 1-1-1 Honjo, Kumamoto 860-0811, Japan
Y Ando, M Nakamura, Department of Diagnostic Medicine, Graduate School of Medical Sciences, Kumamoto University, 1-1-1 Honjo, Kumamoto 860-0811, Japan
K Kitagawa, Department of Ophthalmology, Kanazawa Medical University Hospital, 1-1 Daigaku, Uchinada-machi, Kahoku-gun, Ishikawa 920-0293, Japan
S Ikemizu, Department of Structural Biology, Graduate School of Medical Sciences, Kumamoto University, 1-1-1 Honjo, Kumamoto 860-0811, Japan
T Yamashita, M Ueda, Department of Neurology, Graduate School of Medical Sciences, Kumamoto University, 1-1-1 Honjo, Kumamoto 860-0811, Japan
K Hirano, Department of Ophthalmology, Japanese Red Cross Nagoya First Hospital, 3-35 Michishita-cho, Nagoya 453-8511, Japan
M Yamada, Division for Vision Research, National Institute of Sensory Organs, National Tokyo Medical Center, 2-5-1 Higashigaoka, Meguro 152-8902, Tokyo, Japan
S Kinoshita, Department of Ophthalmology, Kyoto Prefectural University of Medicine, 465 Kajii-cho, Kawaramachidori Noboru, Kamigyoku, Kyoto 602-8566, Japan

Competing interests: The authors have no proprietary, financial, or commercial interests in any of the companies or products mentioned in this paper.

REFERENCES

1 **Glenner GG**, Page DL. Amyloid, amyloidosis, and amyloidogenesis. *Int Rev Exp Pathol* 1976;**15**:1–92.
2 **Tan SY**, Pepys MB. Amyloidosis. *Histopathology* 1994;**25**:403–14.
3 **Westermark P**, Benson MD, Buxbaum JN, *et al.* Amyloid fibril protein nomenclature—2002. *Amyloid* 2002;**9**:197–200.
4 **Gorevic PD**, Munoz PC, Gorgone G, *et al.* Amyloidosis due to a mutation of the gelsolin gene in an American family with lattice corneal dystrophy type II. *N Engl J Med* 1991;**325**:1780–5.
5 **Colon W**, Lai Z, McCutchen SL, *et al.* FAP mutations destabilize transthyretin facilitating conformational changes required for amyloid formation. *Ciba Found Symp* 1996;**199**:228–38.
6 **Goldsteins G**, Persson H, Andersson K, *et al.* Exposure of cryptic epitopes on transthyretin only in amyloid and in amyloidogenic mutants. *Proc Natl Acad Sci USA* 1999;**96**:3108–13.
7 **Sandgren O.** Ocular amyloidosis. with special reference to the hereditary forms with vitreous involvement. *Surv Ophthalmol* 1995;**40**:173–96.
8 **Ando E**, Ando Y, Okamura R, *et al.* Ocular manifestation of familial amyloidotic polyneuropathy type I: long term follow up. *Br J Ophthalmol* 1997;**81**:295–8.
9 **Rodrigues M**, Zimmerman LE. Secondary amyloidosis in ocular leprosy. *Arch Ophthalmol* 1971;**85**:277–9.
10 **Hayasaka S**, Setogawa T, Ohmura M. Secondary localized amyloidosis of the cornea caused by trichiasis. *Ophthalmologica* 1987;**194**:77–81.
11 **Watts J**, Frank H. Corneal amyloidosis. *Br J Ophthalmol* 1989;**73**:674–6.
12 **Hill JC**, Maske R, Bowen RM. Secondary localized amyloidosis of the cornea associated with tertiary syphilis. *Cornea* 1990;**9**:98–101.
13 **Dutt S**, Elner VM, Soong HK, *et al.* Secondary localized amyloidosis in interstitial keratitis. Clinicopathologic findings. *Ophthalmology* 1992;**99**:817–23.
14 **Aso K**, Wakakura M. Corneal amyloidosis complicated by trichiasis. Immunohistochemical identification of the amyloid light chain protein. *Jpn J Ophthalmol* 2000;**44**:191.
15 **Kigasawa K**, Mashima Y, Ogata T, *et al.* A histopathological study of corneal amyloidosis secondary to trichiasis. *Nippon Ganka Gakkai Zasshi* 1996;**100**:394–400.
16 **Ando Y**, Nakamura M, Kai H, *et al.* A novel localized amyloidosis associated with lactoferrin in the cornea. *Lab Invest* 2002;**82**:757–66.
17 **Okuda T**, Matsumoto K, Ando Y, *et al.* A case of corneal lactoferrin amyloidosis secondary to trichiasis. *Nippon Ganka Gakkai Zasshi* 2003;**107**:105–8.
18 **Madisen L**, Hoar DI, Holroyd CD, *et al.* DNA banking: the effects of storage of blood and isolated DNA on the integrity of DNA. *Am J Med Genet* 1987;**27**:379–90.
19 **Orita M**, Suzuki Y, Sekiya T, *et al.* Rapid and sensitive detection of point mutations and DNA polymorphisms using the polymerase chain reaction. *Genomics* 1989;**5**:874–9.
20 **Kim SJ**, Yu DY, Pak KW, *et al.* Structure of the human lactoferrin gene and its chromosomal localization. *Mol Cells* 1998;**8**:663–8.
21 **El-Salhy M**, Suhr O. Endocrine cells in rectal biopsies from patients with familial amyloidotic polyneuropathy. *Scand J Gastroenterol* 1996;**31**:68–73.
22 **Klintworth GK**, Valnickova Z, Kielar RA, *et al.* Familial subepithelial corneal amyloidosis-a lactoferrin-related amyloidosis. *Invest Ophthalmol Vis Sci* 1997;**38**:2756–63.
23 **Baker EN**, Anderson BF, Baker HM, *et al.* Three-dimensional structure of lactoferrin. Implications for function, including comparisons with transferrin. *Adv Exp Med Biol* 1998;**443**:1–14.
24 **Tsunoda I**, Awano H, Kayama H, *et al.* Idiopathic AA amyloidosis manifested by autonomic neuropathy, vestibulocochleopathy, and lattice corneal dystrophy. *J Neurol Neurosurg Psychiatry* 1994;**57**:635–7.
25 **Tsujikawa M**, Kurahashi H, Tanaka T, *et al.* Identification of the gene responsible for gelatinous drop-like corneal dystrophy. *Nat Genet* 1999;**21**:420–3.
26 **Tasa G**, Kals J, Muru K, *et al.* A novel mutation in the M1S1 gene responsible for gelatinous droplike corneal dystrophy. *Invest Ophthalmol Vis Sci* 2001;**42**:2762–4.
27 **Stewart H**, Black GC, Donnai D, *et al.* A mutation within exon 14 of the TGFBI (BIGH3) gene on chromosome 5q31 causes an asymmetric, late-onset form of lattice corneal dystrophy. *Ophthalmology* 1999;**106**:964–70.

Ocular decompression retinopathy following trabeculectomy with mitomycin C associated with familial amyloidotic polyneuropathy

M Wakita, T Kawaji, E Ando, T Koga, M Inatani, H Tanihara and Y Ando

Br. J. Ophthalmol. 2006;90;515-516
doi:10.1136/bjo.2005.082735

Another feature of CGD involves poor wound healing.[10] Therefore, subretinal granulation tissue mass in our case may represent an abnormal reparative response to previous chorioretinal injury. The absence of infection or granuloma, intravitreal pro-inflammatory cytokines, and improvement with immunosuppression suggests that his ocular disease is probably the result of aberrant inflammatory responses. Routine ocular biopsy is not recommended as part of standard ophthalmic evaluation.

R R Buggage
Laboratory of Immunology, National Eye Institute, National Institute of Allergy and Infectious Diseases, National Institutes of Health, Bethesda, MD, USA

R M Bauer II
Winn Army Hospital, Fort Stewart, GA, USA

S M Holland
Laboratory of Host Defenses, National Institute of Allergy and Infectious Diseases, National Institutes of Health, Bethesda, MD, USA

C I Santos
Department of Ophthalmology, University of Puerto Rico, San Juan, Puerto Rico

C-C Chan
Laboratory of Immunology, National Eye Institute, National Institute of Allergy and Infectious Diseases, National Institutes of Health, Bethesda, MD, USA

Correspondence to: Chi-Chao Chan, MD, National Eye Institute, National Institutes of Health, 10 Center Drive, Bldg 10, Room 10N103, Bethesda, MD 20892-1857, USA; chanc@nei.nih.gov

doi: 10.1136/bjo.2005.081505

Accepted for publication 1 November 2005

Financial support: Intramural program of the National Eye Institute, NIH.

References

1 **Segal BH**, Leto TL, Gallin JI, *et al*. Genetic, biochemical, and clinical features of chronic granulomatous disease. *Medicine (Baltimore)* 2000;**79**:170–200.
2 **Johnston RB Jr**. Clinical aspects of chronic granulomatous disease. *Curr Opin Hematol* 2001;**8**:17–22.
3 **El-Benna J**, Dang PM, Gougerot-Pocidalo MA, *et al*. Phagocyte NADPH oxidase: a multicomponent enzyme essential for host defenses. *Arch Immunol Ther Exp (Warsz)* 2005;**53**:199–206.
4 **Clark RA**, Malech HL, Gallin JI, *et al*. Genetic variants of chronic granulomatous disease: prevalence of deficiencies of two cytosolic components of the NADPH oxidase system. *N Engl J Med* 1989;**321**:647–52.
5 **Palestine AG**, Meyers SM, Fauci AS, *et al*. Ocular findings in patients with neutrophil dysfunction. *Am J Ophthalmol* 1983;**95**:598–604.
6 **Goldblatt D**, Butcher J, Thrasher AJ, *et al*. Chorioretinal lesions in patients and carriers of chronic granulomatous disease. *J Pediatr* 1999;**134**:780–3.
7 **Djalilian AR**, Smith JA, Walsh TJ, *et al*. Keratitis caused by Candida glabrata in a patient with chronic granulomatous disease. *Am J Ophthalmol* 2001;**132**:782–3.
8 **Valluri S**, Chu FC, Smith ME. Ocular pathologic findings of chronic granulomatous disease of childhood. *Am J Ophthalmol* 1995;**120**:120–3.
9 **Grossniklaus HE**, Frank KE, Jacobs G. Chorioretinal lesions in chronic granulomatous disease of childhood. Clinicopathologic correlations. *Retina* 1988;**8**:270–4.
10 **Eckert JW**, Abramson SL, Starke J, *et al*. The surgical implications of chronic granulomatous disease. *Am J Surg* 1995;**169**:320–3.

Ocular decompression retinopathy following trabeculectomy with mitomycin C associated with familial amyloidotic polyneuropathy

Familial amyloidotic polyneuropathy (FAP), a disorder inherited in autosomal dominant fashion, is characterised by systemic accumulation of polymerised mutated amyloidogenic TTR (ATTR) in peripheral nerves and in organs.[1] We report two patients with FAP ATTR Y114C (a point mutation, from tyrosine to cysteine, at codon 114) who developed diffuse retinal haemorrhages immediately after uncomplicated trabeculectomy with mitomycin C (MMC).

Case reports

A woman underwent vitrectomy for vitreous opacity associated with FAP ATTR Y114C in the left eye when she was 34 years old and in the right eye when she was 35 years old. Neurological examination revealed that she had polyneuropathy and autonomic dysfunction, and she underwent liver transplantation at 34 years old. Thereafter, intraocular pressure (IOP) in the left eye gradually increased and visual field loss progressed. Trabeculectomy with MMC in the left eye was performed when she was 39 years old. Preoperative IOP was 43 mm Hg despite maximal medical therapy. On the next postoperative day, IOP was 5 mm Hg, and fundus examination revealed scatter retinal haemorrhages in the periphery and posterior pole (fig 1). The haemorrhages had completely resolved and visual acuity was 20/20 in the left eye.

A woman underwent vitrectomy for vitreous opacity associated with FAP ATTR Y114C when she was 45 and trabeculectomy in the right eye at another hospital when she was 46, respectively. At 48, vitrectomy in the left eye was performed. She underwent liver transplantation at 50. Thereafter, IOP in the left eye gradually increased and non-penetrating trabeculectomy with MMC was performed when she was 51. However, IOP increased postoperatively, and trabeculectomy with MMC was added. IOP before the additional trabeculectomy was 37 mm Hg despite maximal medical therapy. On the next postoperative day, IOP was 5 mm Hg, and fundus examination revealed scatter retinal haemorrhages in the periphery and posterior pole involving the fovea. Although haemorrhages had almost resolved during the follow up period, visual acuity decreased from 20/20 to 20/50.

Comment

Retinal haemorrhages are a rare complication after filtration surgery.[2 6] Fechtner *et al* reported this condition for the first time under the descriptive term of ocular decompression retinopathy.[2] Affected patients are typically young, but not exclusively, with relatively high preoperative IOP, a very low postoperative IOP, and advanced cupping. Elevated IOP levels are generally significantly high in cases of secondary glaucoma related to FAP,[7] and diffuse retinal haemorrhages immediately after uncomplicated trabeculectomy with MMC are noted in both cases. One possible mechanism is hypothesised to be caused by a loss of autoregulation of retinal vessels, which overwhelms their capacity to respond to changes in IOP, resulting in retinal haemorrhages.[2] Our cases had an autonomic dysfunction as a systemic symptom, further increasing the susceptibility to such a phenomenon. Also, although both

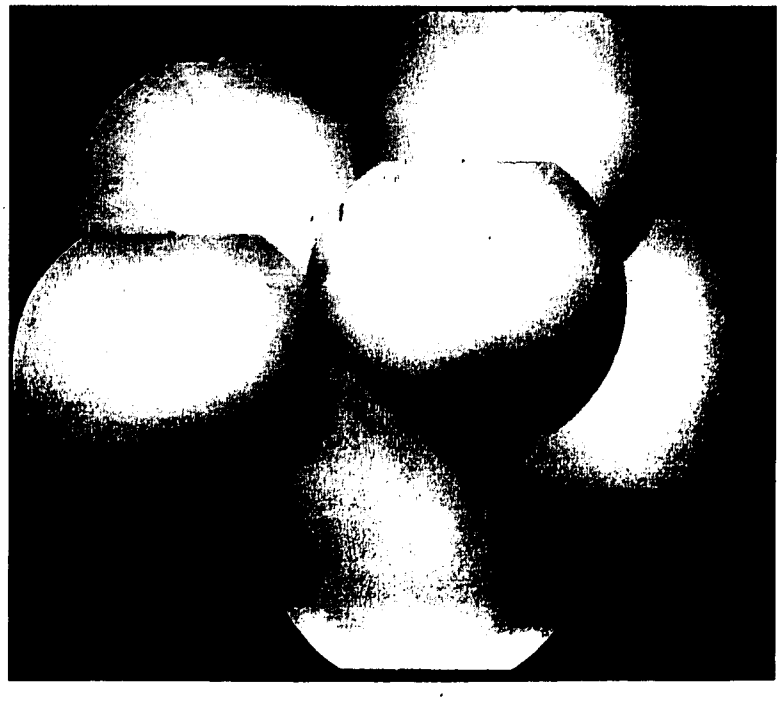

Figure 1 Scatter retinal haemorrhages in the periphery and posterior pole on the first postoperative day.

cases underwent trabeculectomy after vitrectomy, there were no complications, such as the collapse of eye, caused by a vitreous condition. Visual prognosis is usually benign after the resolution of haemorrhages; however, cases with poor visual acuity as shown in case 2 have also been described. Taken together, because clinical features in glaucoma secondary to FAP are related to the pathogenesis of this rare complication after trabeculectomy, early postoperative hypotony should be avoided to prevent it.

Acknowledgements

The authors' work was supported in part by a grant in aid for scientific research from the Ministry of Education, Science, Sports and Culture, Japan, from the Ministry of Health and Welfare, Japan.

M Wakita, T Kawaji, E Ando, T Koga, M Inatani, H Tanihara
Department of Ophthalmology and Visual Science, Graduate School of Medical Sciences, Kumamoto University, 1-1-1 Honjo, Kumamoto 860-8556, Japan

Y Ando
Department of Diagnostic Medicine, Graduate School of Medical Sciences, Kumamoto University, 1-1-1 Honjo, Kumamoto 860-8556, Japan

Correspondence to: Takahiro Kawaji, MD, Ophthalmology and Visual Science, Graduate School of Medical Sciences, Kumamoto University, 1-1-1 Honjo, Kumamoto 860-8556, Japan; kawag@white.plala.or.jp

doi: 10.1136/bjo.2005.082735

Accepted for publication 1 November 2005

References

1 **Araki S.** [Type I familial amyloidotic polyneuropathy]. *No To Hattatsu* 1984;**16**:92–100.
2 **Fechtner RD**, Minckler D, Weinreb RN, *et al.* Complications of glaucoma surgery. Ocular decompression retinopathy. *Arch Ophthalmol* 1992;**110**:965–8.
3 **Dudley DF**, Leen MM, Kinyoun JL, *et al.* Retinal hemorrhages associated with ocular decompression after glaucoma surgery. *Ophthalmic Surg Lasers* 1996;**27**:147–50.
4 **Suzuki R**, Nakayama M, Satoh N. Three types of retinal bleeding as a complication of hypotony after trabeculectomy. *Ophthalmologica* 1999;**213**:135–8.
5 **Danias J**, Rosenbaum J, Podos SM. Diffuse retinal hemorrhages (ocular decompression syndrome) after trabeculectomy with mitomycin C for neovascular glaucoma. *Acta Ophthalmol Scand* 2000;**78**:468–9.
6 **Dev S**, Herndon L, Shields MB. Retinal vein occlusion after trabeculectomy with mitomycin C. *Am J Ophthalmol* 1996;**122**:574–5.
7 **Kimura A**, Ando E, Fukushima M, *et al.* Secondary glaucoma in patients with familial amyloidotic polyneuropathy. *Arch Ophthalmol* 2003;**121**:351–6.

Dapsone induced haemolytic anaemia in patients treated for ocular cicatricial pemphigoid

Ocular cicatricial pemphigoid (OCP) is a systemic autoimmune disease of unknown aetiology. It causes a chronic, scarring conjunctivitis and frequently affects other mucous membranes. Definitive diagnosis is made by immunofluorescent staining of conjunctival tissue demonstrating IgG, IgM, and or IgA in the basement membrane. Dapsone is an immunomodulating sulphonamide and has widely been used in the treatment of mild to moderate OCP.[2 4] All patients treated with dapsone show varying degrees of haemolysis.[5] Haemolytic anaemia, requiring withdrawal of therapy, has been shown to occur in approximately 10% of patients.[2 5]

The medical records of 12 patients treated with dapsone for ocular cicatricial disease were reviewed. Eleven of these patients were treated with dapsone as first line therapy and one as second line therapy; 11 patients had ocular cicatricial pemphigoid (OCP) and one had idiopathic cicatrising disease. There were an equal number of male and females in this group with a mean age of 72 years (range 55–89 years). The daily dose of dapsone was consistent at 50 mg twice daily taken orally. Mean follow up time while on dapsone therapy was 19 months with a range of 1–60 months.

Six (50%) patients had reticulocytosis including four (33%) with clinically significant haemolytic anaemia with a raised mean cell volume and a steady fall in haemoglobin from baseline. The development of the haemolytic anaemia was not dose dependent and all the patients had a diagnosis of OCP (table 1).

Our cohort of patients had a much higher rate of haemolytic anaemia than previously published reports.[2 5] Although our study sample is small, the proportion of patients with haemolytic anameia is striking. Patients who are glucose-6-phosphate hydrogenase (G6PD) deficient are known to be more at risk of developing haemolytic anaemia.[4] We do not routinely check for this rare deficiency in our department. Clinically significant dapsone induced haemolytic anaemia may occur more frequently than previously expected and clinicians should be acutely aware of any downward trend in haemoglobin from baseline. We no longer use dapsone as a first line agent in the management of OCP.

M S Wertheim, J J Males, S D Cook, D M Tole
Bristol Eye Hospital, Lower Maudlin Street, Bristol BS1 2LX, UK

Correspondence to: Michael S Wertheim, Bristol Eye Hospital, Lower Maudlin Street, Bristol BS1 2LX, UK; drwertie@hotmail.com

doi: 10.1136/bjo.2005.085837

Accepted for publication 3 December 2005

The authors have no competing interests.

References

1 **Chiou AG**, Florakis GJ, Kazim M. Management of conjunctival cicatrizing diseases and severe ocular surface dysfunction. *Surv Ophthalmol* 1998;**43**:19–46.
2 **Doan S**, Lerouic JF, Robin H, *et al.* Treatment of ocular cicatricial pemphigoid with sulfasalazine. *Ophthalmology* 2001;**108**:1565–8.
3 **Rogers RS 3rd**, Seehafer JR, Perry HO. reatment of cicatricial (benign mucous membrane) pemphigoid with dapsone. *J Am Acad Dermatol* 1982;**6**:215–23.
4 **Tauber J**, Sainz de la Maza M, Foster CS. Systemic chemotherapy for ocular cicatricial pemphigoid. *Cornea* 1991;**10**:185–95.
5 **Foster CS**. Cicatricial pemphigoid. *Trans Am Ophthalmol Soc* 1986;**84**:527–663.

Bilateral juxtapapillary choroidal neovascularisation associated with interferon alfa treatment of a metastatic cutaneous melanoma

Interferon alfa (IFNα) is commonly used in the treatment of many neoplastic diseases owing to its antiproliferative and immunomodulatory effects. IFNα is used in adjuvant therapy of melanoma stage IIa/b or higher.[1] A wide variety of ocular adverse events related to IFN therapy have been reported during the past decades.[2 3] A case of bilateral juxtapapillary choroidal neovascularisation is described here.

Case report

A 48 year old woman reported acute vision loss in her left eye (LE) 1 week after starting treatment with IFNα for a cutaneous metastasic melanoma. She had been receiving IFNα, 5 million international units (MIU), subcutaneously three times a week. On examination, visual acuity (VA) was right eye (RE) 20/50 and LE 20/60. Funduscopy showed bilateral optic disc oedema and subretinal haemorrhages in inferior temporal and nasal arcades. To rule out any cause of papilloedema a brain computed tomography was performed, which was normal. One month later, IFNα doses were increased to 8 MIU; VA decreased to RE 20/100 and LE counting fingers at 9 feet. Funduscopy showed bilateral optic disc oedema, bilateral juxtapapillary serous retinal detachment, and subretinal haemorrhages (fig 1A, B).

Table 1 Patients with haematological complications from dapsone

Patient	Age (years)	Sex	Diagnosis	Dapsone dose	Complication
1	77	M	OCP	50 mg twice daily	Reticulocytosis (with normal Hb)
2	78	M	OCP	50 mg twice daily	Haemolytic anaemia*
3	67	M	OCP	50 mg twice daily	Reticulocytosis (with normal Hb)
4	60	F	OCP	50 mg twice daily	Haemolytic anaemia*
5	89	F	OCP	50 mg twice daily	Haemolytic anaemia*
6	85	F	OCP	50 mg twice daily	Haemolytic anaemia*

OCP, ocular cicatricial pemphigoid, Hb, haemoglobin, *dapsone withdrawn.

Available online at www.sciencedirect.com
SCIENCE DIRECT
Experimental Eye Research 81 (2005) 306–312
EXPERIMENTAL EYE RESEARCH
www.elsevier.com/locate/yexer

Transthyretin synthesis in rabbit ciliary pigment epithelium

Takahiro Kawaji[a], Yukio Ando[b,*], Masaaki Nakamura[b], Keiichi Yamamoto[b], Eiko Ando[a], Akiomi Takano[a], Yasuya Inomata[a], Akira Hirata[a], Hidenobu Tanihara[a]

[a]*Department of Ophthalmology and Visual Science, Graduate School of Medical Sciences, Kumamoto University, 1-1-1 Honjo, Kumamoto 860-8556, Japan*
[b]*Department of Diagnostic Medicine, Graduate School of Medical Sciences, Kumamoto University, 1-1-1 Honjo, Kumamoto 860-8556, Japan*

Received 1 August 2004; accepted in revised form 7 February 2005
Available online 9 March 2005

Abstract

Ocular symptoms of transthyretin (TTR)-related familial amyloidotic polyneuropathy (FAP) suggest that ciliary pigment epithelium (CPE) may synthesize TTR and its TTR may lead to amyloid formation in addition to TTR from vessels and retinal pigment epithelium (RPE). To clarify sites of TTR synthesis in ocular tissues, we performed in situ hybridization and reverse transcription-polymerase chain reaction (RT-PCR) for qualitative detection of TTR mRNA. In addition, we quantified levels of TTR mRNA expression by means of real-time quantitative RT-PCR. Furthermore, although TTR is an anti-acute phase protein in serum level, no reports on changes in TTR expression in ocular tissues during acute inflammation exist. To investigate changes in TTR expression in ocular tissues during inflammation, we induced uveitis by endotoxin challenge in rabbits and used real-time quantitative RT-PCR to examine changes in TTR mRNA expression in ocular tissues. In situ hybridization and RT-PCR qualitatively demonstrated TTR mRNA not only in RPE but also in CPE. Real-time quantitative RT-PCR showed that the level of TTR mRNA expression in the CPE was about one-third of that in the RPE. TTR mRNA expression in ocular tissues decreased as the degree of inflammation increased. These results suggest that TTR synthesized in the CPE may lead to ocular manifestations, especially glaucoma, in FAP. TTR mRNA also acts as an anti-acute phase reactant in ocular tissues.

Keywords: transthyretin; ciliary epithelium; familial amyloidotic polyneuropathy; glaucoma; anti-acute phase protein

1. Introduction

Transthyretin (TTR)-related familial amyloidotic polyneuropathy (FAP) is an autosomal dominant inherited disorder characterized by systemic accumulation of polymerized mutated TTR in the peripheral nerves and other organs, such as autonomic nervous system, choroid plexus, cardiovascular system, kidney, thyroid, gastrointestinal tract and eye (Ando et al., 1992). More than 100 different point mutations in the gene, most of which lead to production of amyloidogenic TTR (ATTR), have been identified in patients with FAP (Connors et al., 2003). In various types of FAP, ocular manifestations are commonly found although amyloid formation mechanism in ocular tissues as well as other systemic organs remains to be elucidated.

TTR is a 55-kDa tetramer protein in which each subunit is composed of 127 amino acids (Kanda et al., 1974). The main source of plasma TTR has been documented to be the liver (Felding and Fex, 1982), but the retinal pigment epithelium (RPE) (Martone et al., 1988; Cavallaro et al., 1990), the choroid plexus of the brain (Dickson et al., 1985; Soprano et al., 1985; Herbert et al., 1986) and the visceral yolk sac endoderm (Soprano et al., 1986) are also known to synthesize TTR. Furthermore, TTR protein had been detected in number of ocular tissues: RPE, retinal ganglion cells, nerve fiber layer of the retina, photoreceptor layer, ciliary epithelium, iris epithelium, lens capsule, corneal endothelium, and lacrimal glandular epithelium (Inada, 1988; Dwork et al., 1990). It plays an important role in plasma transport of thyroxin and, through its interaction with serum retinol-binding protein, of retinol (van Jaarsveld et al., 1973). The protein is an anti-acute phase protein whose serum levels decrease during acute inflammation, infection, and surgical stress. However, no reports on

* Corresponding author. Dr Yukio Ando, Department of Diagnostic Medicine, Graduate School of Medical Sciences, Kumamoto University, 1-1-1 Honjo, Kumamoto 860-8556, Japan.
E-mail address: yukio@kaiju.medic.kumamoto-u.ac.jp (Y. Ando).

0014-4835/$ - see front matter © 2005 Elsevier Ltd. All rights reserved.
doi:10.1016/j.exer.2005.02.003

changes in TTR expression in ocular tissues in such pathologic conditions exist.

Most FAP patients with secondary glaucoma have vitreous opacities, dandruff-like substances on the lens surface or pupillary margin, and pigment deposition in the chamber angle (Kimura et al., 2003). This evidence led to the common belief that ocular amyloid deposition originating from the vessels and the RPE may result in obstruction of the aqueous outflow route (Silva-Araujo et al., 1993). However, because we had observed several FAP patients who had glaucoma with severe amyloid deposition on the pupil and pupil fringe with little or no vitreous opacity (Futa et al., 1984), thus making this hypothesis less likely. TTR synthesized by sites other than the RPE in ocular tissues, sites close to the chamber angle, may predominantly cause glaucoma with amyloid deposition on the pupil and pupil fringe in such cases. We believed that one possibility would be additional TTR expression in ciliary pigment epithelium (CPE) cells, which, like the RPE cells, are differentiated from the outer layer of the embryologic optic cup.

In the present study, we clarified sites of TTR synthesis in ocular tissues in addition to the RPE and investigated the effect of inflammation on the change in TTR expression in ocular tissues by inducing uveitis in endotoxin-challenged rabbits.

2. Materials and methods

2.1. Animals

Japanese adult albino male rabbits (Kyudo Co., Kumamoto, Japan), 12 weeks of age and each weighing about 2·0–2·5 kg, were used in this study. The animals were treated in accordance with the ARVO Statement for the Use of Animals in Ophthalmic and Vision Research and the guidelines of the Committee on Animal Research of Kumamoto University.

2.2. Tissue preparation

The animals were killed by using an intravenously injected overdose of pentobarbital. Ten eyes were enucleated immediately and fixed overnight in a mixture of 4% paraformaldehyde in 0·1 M phosphate buffer at 4°C. The eyes were cut circumferentially at the cornea (2–3 mm anterior from the limbus) to remove the cornea and lens to make posterior cups, and samples were embedded in paraffin. These samples were used for in situ hybridization, reverse transcription-polymerase chain reaction (RT-PCR) analysis and real-time quantitative RT-PCR analysis. Forty eyes were cut circumferentially at the sclera (1 mm posterior from the limbus) to make anterior cups without RPE and posterior cups. CPE and RPE were obtained via dissection directly from anterior cups and posterior cups, respectively. These fresh tissues were frozen immediately with liquid nitrogen and stored at −80°C until use for real-time quantitative RT-PCR analysis.

2.3. Preparation of probes

Rabbit TTR cDNA samples were amplified by use of RT-PCR with rabbit liver mRNA, and cDNA was cloned into pDrive Cloning Vector (Qiagen, Tokyo, Japan). Plasmid templates were linearized, and fluorescein-substituted antisense and sense RNA probes were transcribed by using Fluorescein RNA Labeling Mix (Roche Diagnostics GmbH, Penzberg, Germany) and DIG RNA Labeling Mix (Roche Diagnostics GmbH), according to the manufacturer's protocols.

2.4. In situ hybridization

In situ hybridization was performed with a tyramide signal amplification system with fluorescein-labeled probes (GenPoint Fluorescein; Dako, Carpinteria) according to the manufacturer's instructions with a slight modification. Before hybridization, paraffin-embedded sections were immersed in three changes of xylene for 5 min. Residual xylene was removed by immersing the sections in two changes of 99% ethanol, followed by two changes of 95% ethanol, for each 3 min. Sections were then rehydrated with several changes of water and were pretreated with proteinase K (20 $\mu g\,mL^{-1}$) at room temperature (RT) for 10 min. After sections were washed with Tris–buffered saline/Tween (TBST), they were passed through a graded ethanol series (70, 95, and 99%). Hybridization in mRNA in situ hybridization solution (Dako, Carpinteria), containing 0·2 $\mu g\,mL^{-1}$ fluorescein-labeled RNA probes, which was preheated at 80°C, continued overnight at 45°C. After the sections were washed with the stringent wash solution twice at 55°C for 20 min and with TBST for 5 min, they were covered by 3% hydrogen peroxide at RT for 5 min. Samples were washed with TBST twice for 3 min, and then the antibody was incubated in anti-fluorescein isothiocyanate (FITC)-horseradish peroxidase (HRP) solution (×100 dilution) for 30 min at RT. After sections were washed three times with TBST for 3 min, they were covered by fluorescyl tyramide solution at RT for 15 min. Sections were washed again three times with the TBST for 3 min, and then anti-FITC-HRP solution was added to the sections at RT for 30 min. Sections were then washed three times with TBST for another 3 min, after which the sections were covered for 15 sec with 3,3′-diaminobenzidine chromogen with buffered solution containing hydrogen peroxide. The reaction was stopped by immersing the sections in water for 1 min. Sections were then viewed under the light microscope and photographed.

2.5. Isolation of RNA from targeted tissue areas and qualitative RT-PCR

To obtain pure CPE without RPE, we used the Pinpoint Slide RNA Isolation System II (Zymo Research, Orange) and isolated RNA from specific paraffin-embedded tissue areas on slides, according to the manufacturer's instructions.

RT-PCR was performed with SuperScript One-Step RT-PCR with Platinum Taq (Invitrogen, Carlsbad), according to the manufacturer's protocols. For the RT-PCR analysis, 1 μg of template RNA, 0·2 μM sense primers, 0·2 μM antisense primers, 1 μL of RT/Platinum Taq Mix, and 25 μL of 2× reaction mixture in a total volume of 50 μL were used. The primers were designed for spanning between exon 2 and exon 3 so that cDNA fragments were easily distinguishable from genomic fragments. RNA was reverse-transcribed into cDNA by one cycle at 50°C for 30 min followed by one cycle at 94°C for 2 min. The cDNA was amplified for 36 cycles: 94°C for 15 sec, 50°C for 30 sec, and 72°C for 1 min (the last cycle at 72°C for 5 min). After amplification, PCR products were run on 1·2% agarose gel, stained with ethidium bromide, and photographed with Printgraph (model AE-6911, ATTO, Tokyo, Japan), and the photographs were saved via Image Saver (model AE-6905, ATTO).

2.6. Real-time quantitative RT-PCR

Total RNA for analysis of TTR mRNA level on RPE cells and CPE cells was prepared from paraffin-embedded tissue samples by using Pinpoint Slide RNA Isolation System II and frozen tissue samples by using AquaPure RNA Isolation Kit (Bio-Rad, Hercules) according to the manufacturer's instructions. Total RNA for analysis of endotoxin-induced uveitis (EIU) model was prepared from frozen tissue samples by using AquaPure RNA Isolation Kit according to the manufacturer's instructions. The LightCycler RNA Master Hybridization Probe (Roche Diagnostics GmbH) is a specifically adapted product for one-step RT-PCR in glass capillaries using the LightCycler instrument and hybridization probes for detection. Real-time one-step PCR for TTR mRNA in rabbits was performed by using a LightCycler thermal cycling system according to the manufacturer's instructions. Glucose-6-phosphate dehydrogenase (G6PD) was used as internal control. The data for quantification were analysed with the LightCycler analysis software. TTR mRNA levels were estimated as the ratio of rabbit TTR mRNA copies to G6PD mRNA copies.

2.7. Generation of endotoxin-induced uveitis in rabbits

Lipopolysaccharide (LPS) from *Salmonella typhimurium* (Sigma, St Louis, MO) was dissolved in sterile phosphate-buffered saline (PBS) at a concentration of 1 mg mL^{-1}. Rabbits were anesthetized with intravenous pentobarbital (Nembutal; Dainippon Pharmaceuticals, Osaka, Japan) and intramuscular ketamine hydrochloride (Ketaral 50; Sankyo Pharmaceuticals, Tokyo, Japan). The pupils were dilated with a mixture of 0·5% tropicamide and 0·5% phenylephrine hydrochloride. A 30-gauge needle was inserted transconjunctivally at the temporal side (2–3 mm posterior to the limbus) with the aid of a surgical microscope. For each rabbit, 50 μg of LPS was injected into the vitreous cavity in one eye and 50 μL of PBS was administered to the other eye as the control.

Signs of uveitis were observed by slit lamp examinations at 3, 6, 12, 24, and 48 hr after LPS injection. The severity of the EIU was graded from 0 to 4 according to a previous definition (Ruiz-Moreno et al., 1992): 0, no inflammatory reaction; 1, discrete inflammatory reaction; 2, moderate dilation of the iris and conjunctival vessels; 3, intense iridal hyperemia with flare in the anterior chamber; and 4, same clinical signs as 3 plus presence of fibrinoid exudation in the papillary area with intense flare in the anterior chamber. Changes in TTR mRNA in the CPE and RPE were evaluated by real-time quantitative RT-PCR with the LightCycler system.

2.8. Statistical analysis

TTR mRNA levels are expressed as mean ± standard error of mean (S.E.M.). Differences were analysed via the paired *t*-test. Differences were considered significant when $P<0·05$.

3. Results

3.1. In situ hybridization

In situ hybridization assays of the rabbit eye sections with the antisense probe revealed the presence of hybridization signals for TTR mRNA not only within the RPE cells but also the CPE cells (Fig. 1A and C). The signals were distributed uniformly and abundantly within the cytoplasm of all RPE and CPE cells. Control sections hybridized with the sense probe showed no hybridization signal (Fig. 1B and D).

3.2. Isolation of RNA from targeted tissue areas and qualitative RT-PCR

We isolated RNA from specific paraffin-embedded tissue areas on slides (Fig. 2A). We applied the pinpoint solution on the targeted area with the aid of a microscope, which showed clearly that area 1 did not include RPE cells. RT-PCR revealed expression of TTR mRNA in CPE cells. The expression level in the RPE cells was higher than that in the CPE cells (Fig. 2B).

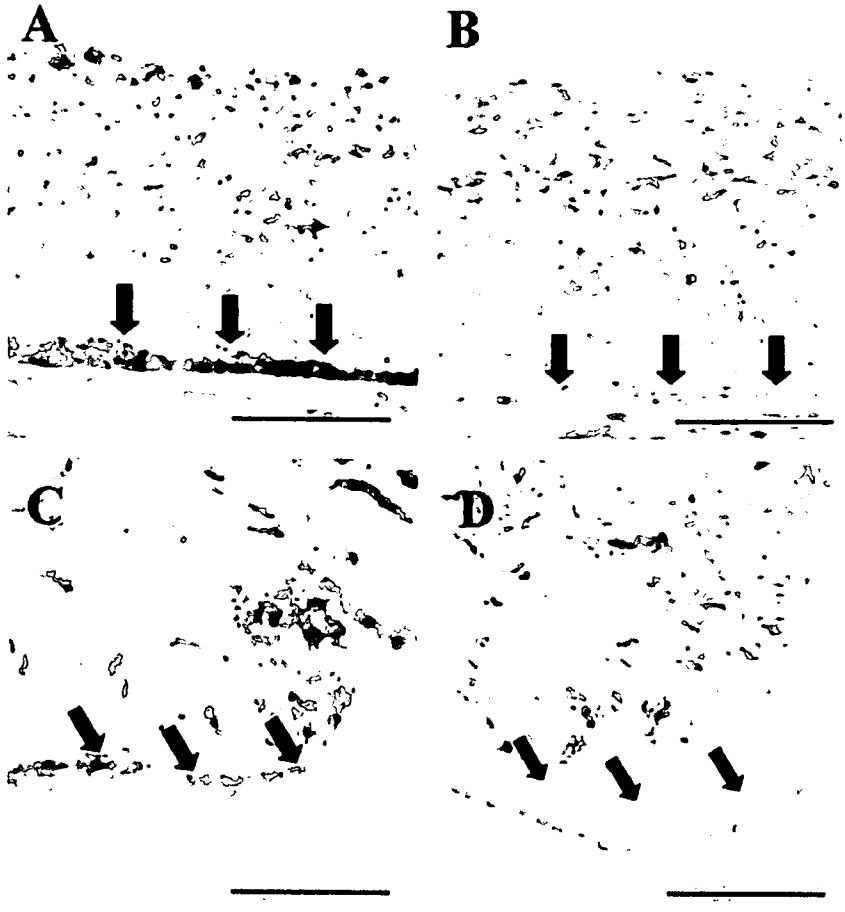

Fig. 1. In situ hybridization studies of rabbit eye sections via a tyramide signal amplification system with a fluorescein-labeled RNA probe for rabbit TTR. The tissues were analysed under light microscopy. Antisense (A) and sense (B) probes in RPE cells; antisense (C) and sense (D) probes in CPE cells. Bar represents 50 μm.

3.3. Real-time quantitative RT-PCR

Real-time quantitative RT-PCR analysis with the LightCycler revealed that the TTR mRNA level in CPE cells was approximately one-third of that in the RPE cells with both paraffin-embedded tissue samples and frozen tissue samples (Fig. 3).

3.4. Real-time quantitative RT-PCR with the EIU Model

Signs of uveitis, such as dilation of the iris and conjunctival vessels, iridial hyperemia, and flare in the anterior chamber, were discovered by means of slit lamp examinations 3 hr after intravitreous LPS injection, and the degree of change continued to increase up to 48 hr. Table 1 shows the time course of EIU grades after LPS injection. Control eyes had no signs of uveitis. Histological examinations showed that the number of inflammatory cells increased in iris and ciliary body, as compared to that seen in retina, in time-dependent manner (Fig. 4). Real-time quantitative RT-PCR analysis with the LightCycler revealed that TTR mRNA levels in the RPE cells decreased slightly until 6 hr after induction of inflammation (Fig. 5). However, at 12 hr and thereafter, TTR mRNA returned to normal levels. TTR mRNA levels in CPE cells were down-regulated by the induced inflammation.

4. Discussion

In this study, we presented new evidence of TTR production in CPE cells by means of qualitative and quantitative methods. In situ hybridization analysis of rabbit eyes revealed the presence of TTR mRNA not only in RPE cells but also in CPE cells. RT-PCR investigations demonstrated that RPE cells expressed higher TTR mRNA levels than did CPE cells. Real-time quantitative RT-PCR studies showed that the level of TTR mRNA expression in CPE cells was about one-third of that in RPE cells. After an inflammatory challenge achieved by intravitreous LPS injection, TTR mRNA levels in RPE cells decreased slightly until 6 hr after injection, but TTR mRNA levels in

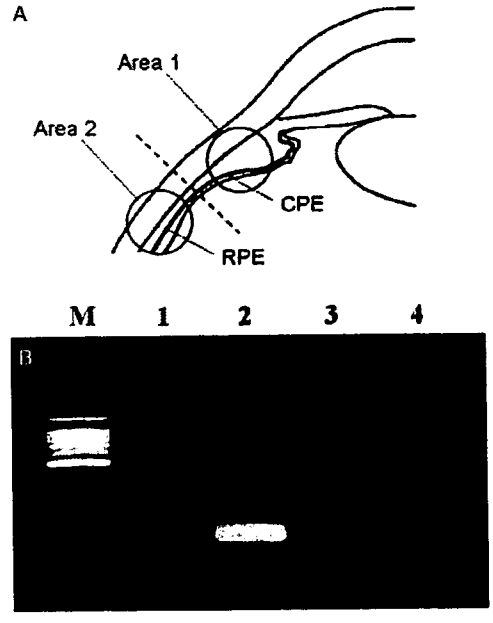

Fig. 2. RNA isolation areas in paraffin-embedded tissue and TTR expression as found in each area via RT-PCR. (A) Areas 1 and 2 included exclusively CPE cells and RPE cells, respectively. (B) Lanes 1 and 3, controls for RPE and CPE cells, respectively, reverse transcription (-); lane 2, RPE cells; lane 4, CPE cells; and lane M, size marker.

CPE cells were significantly down-regulated until 48 hr after injection. The grade of inflammation in around CPE cells was much higher than that in around RPE cells. These results suggest that TTR expression in RPE cells and CPE cells decreased as the degree of inflammation increased.

Our in situ hybridization analysis revealed TTR mRNA expression not only in RPE cells, as previously reported, but also in CPE cells, as we expected. Moreover, we isolated RNA from targeted tissue areas in which CPE cells were included and RPE cells were excluded by using the Pinpoint Slide RNA Isolation System II. Our RT-PCR analysis convincingly confirmed the presence of TTR mRNA expression in CPE cells.

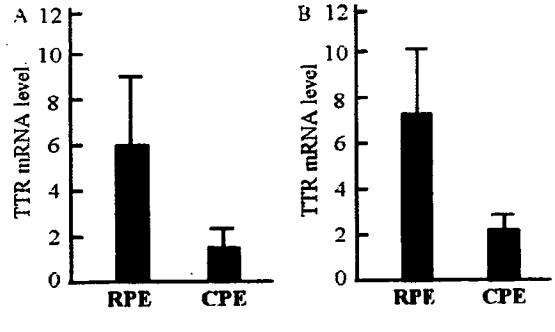

Fig. 3. Expression of TTR mRNA in RPE cells and CPE cells with paraffin-embedded tissue samples (A) and frozen tissue samples (B). The relative levels of mRNA expression were quantified and normalized to levels of G6PD mRNA expression. For each group in paraffin-embedded tissue samples, $n=4$. For each group in frozen tissue samples, $n=7$.

Table 1
Ocular inflammation after LPS injection

Time (hours after LPS injection)	EIU grade[a]
3	1.3
6	2.8
12	4.0
24	4.0
48	4.0

[a] Value represent the mean grade of EIU observed in five rabbits.

Cavallaro et al. (1990) first demonstrated by in situ hybridization methods that, in the rat eye, the RPE was the source of TTR synthesis and that an abrupt demarcation was present between hybridizing and nonhybridizing cells at the junction of the RPE and the CPE. The best possible explanation of the difference between their results and ours may be the sensitivity of the methodology: we used a tyramide signal amplification system with a fluorescein-labeled probe, whereas Cavallaro et al. used a ^{35}S-labeled probe and performed in situ hybridization alone. The sensitivity of the former is much higher than that of the latter (Tani, 1999). Another possibility is the fact that Cavallaro et al. studied rats and we studied rabbit, and that differences could be there purely because of the difference in animal model systems.

Quantitative analysis revealed significant production of TTR in CPE cells, with real-time quantitative RT-PCR demonstrating that the level of TTR mRNA expression in CPE cells was about one-third of that in RPE cells. These results suggest that a part of TTR in aqueous humor may be derived from CPE cells, and TTR synthesized by CPE cells may cause a part of amyloid deposition at the pupillary margin and angle chamber, which would result in glaucoma, while although we really do not know the source of TTR protein in aqueous humor. We accurately excised the tissues, and the reproducibility of the results of ISH and RT-PCR was reliable. Thus, our findings of TTR message in CPE cells does not invalidate our hypothesis that CPE cells is the main source of TTR in FAP patients who had secondary glaucoma with amyloid deposition on the pupil and pupil fringe but with little or no vitreous opacity. On the basis of our present studies, the mechanism of TTR delivery and release should be examined further.

As we described above, ISH and RT-PCR data and clinical evidence may support the contribution of CPE cells to form amyloid fibrils in the pupillary margin and angle chamber, however, ocular biochemical changes in rabbit is different from that in human. Therefore, same analysis should be performed in FAP patients and other animals.

Our study demonstrated that TTR mRNA levels in both CPE and RPE cells were regulated by acute inflammation in ocular tissues. As demonstrated in Fig. 4, the degree of inflammation increased in around CPE cells much higher than in around RPE cells in a time-dependent manner. In contrast, real-time quantitative RT-PCR clearly

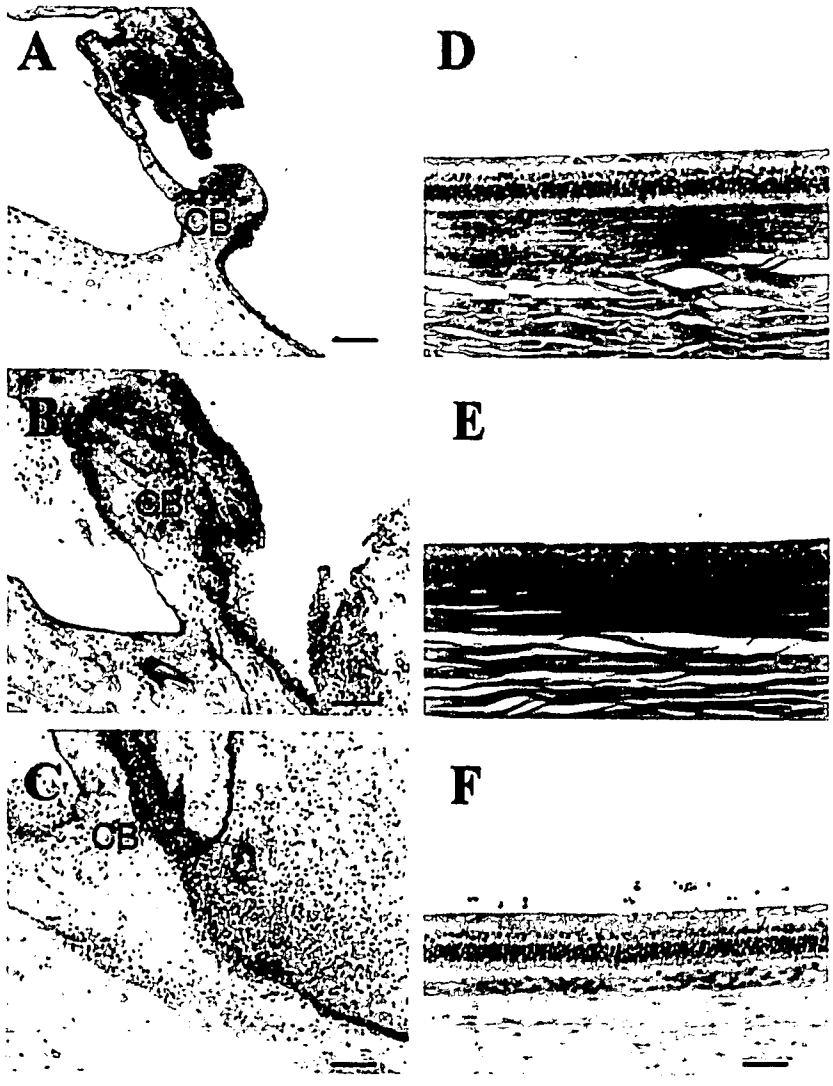

Fig. 4. Light-microscopic photographs of the HE-stained sections of the eyes at 6 (A, D), 12 (B, E) and 48 hr (C, F) after intravitreal LPS injection. Inflammatory cells in ciliary body (A, B, and C) increased much higher than that in retina (D, E, and F) in time-dependent manner. Bar represents 50 μm. CB, ciliary body.

demonstrated that TTR mRNA levels were suppressed, especially in CPE cells for much longer than in RPE cells, which suggests that TTR reacted as anti-acute phase protein in ocular tissues as well as in the liver.

Because TTR is predominantly synthesized by the liver, liver transplantation has been widely accepted as an effective therapy for halting amyloid deposition in systemic tissues (Holmgren et al., 1991; Ando et al., 1995). However, liver transplantation cannot prevent de novo amyloid deposition, and ocular manifestations continue to progress even after the surgery because of TTR synthesis in ocular tissues (Ando et al., 1996, 2000; Munar-Ques et al., 2000; Haraoka et al., 2002). As a result of longer follow-up periods and longer life expectancies of FAP patients, ocular manifestations, especially vitreous opacity and glaucoma, may become more frequent, serious complications for these patients after liver transplantation.

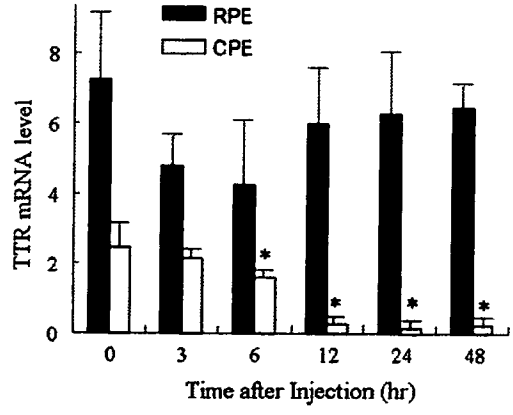

Fig. 5. Changes in TTR mRNA levels in RPE cells and CPE cells 0, 3, 6, 12, 24, and 48 hr after intravitreous LPS injection as described in the text. For each group, $n=5$. $^{*}P<0{\cdot}05$, when compared to normal control (0 hr).

In conclusion, TTR is synthesized by CPE cells as well as RPE cells, whose production of TTR mRNA acts as an anti-acute phase reactant. TTR synthesized by CPE cells may lead to ocular manifestations, especially glaucoma in FAP patients.

Acknowledgements

The authors' work was supported by grants from the Amyloidosis Research Committee, the Pathogenesis, Therapy of Hereditary Neuropathy Research Committee, the Surveys and Research on Specific Disease, the Ministry of Health and Welfare of Japan, Charitable Trust Clinical Pathology Research Foundation of Japan, and Grants-in-Aid for Scientific Research (B) 15390275 from the Ministry of Education, Science, Sports and Culture of Japan.

References

Ando, Y., Araki, S., Shimoda, O., Kano, T., 1992. Role of autonomic nerve functions in patients with familial amyloidotic polyneuropathy as analyzed by laser Doppler flowmetry, capsule hydrograph, and cardiographic R–R interval. Muscle Nerve 15, 507–512.

Ando, Y., Tanaka, Y., Nakazato, M., Ericzon, B.G., Yamashita, T., Tashima, K., Sakashita, N., Suga, M., Uchino, M., Ando, M., 1995. Change in variant transthyretin levels in patients with familial amyloidotic polyneuropathy type I following liver transplantation. Biochem. Biophys. Res. Commun. 211, 354–358.

Ando, Y., Ando, E., Tanaka, Y., Yamashita, T., Tashima, K., Suga, M., Uchino, M., Negi, A., Ando, M., 1996. De novo amyloid synthesis in ocular tissue in familial amyloidotic polyneuropathy after liver transplantation. Transplantation 62, 1037–1038.

Ando, E., Ando, Y., Haraoka, K., 2001. Ocular amyloid involvement after liver transplantation for polyneuropathy. Ann. Intern. Med. 135, 931–932.

Cavallaro, T., Martone, R.L., Dwork, A.J., Schon, E.A., Herbert, J., 1990. The retinal pigment epithelium is the unique site of transthyretin synthesis in the rat eye. Invest. Ophthalmol. Vis. Sci. 31, 497–501.

Connors, L.H., Lim, A., Prokaeva, T., Roskens, V.A., Costello, C.E., 2003. Tabulation of human transthyretin (TTR) variants, 2003. Amyloid 10, 160–184.

Dickson, P.W., Howlett, G.J., Schreiber, G., 1985. Rat transthyretin (prealbumin). Molecular cloning, nucleotide sequence, and gene expression in liver and brain. J. Biol. Chem. 260, 8214–8219.

Dwork, A.J., Cavallaro, T., Martone, R.L., Goodman, D.S., Schon, E.A., Herbert, J., 1990. Distribution of transthyretin in the rat eye. Invest. Ophthalmol. Vis. Sci. 31, 489–496.

Felding, P., Fex, G., 1982. Cellular origin of prealbumin in the rat. Biochim. Biophys. Acta 716, 446–449.

Futa, R., Inada, K., Nakashima, H., Baba, H., Kojima, Y., Okamura, R., Araki, S., 1984. Familial amyloidotic polyneuropathy: ocular manifestations with clinicopathological observation. Jpn. J. Ophthalmol. 28, 289–298.

Haraoka, K., Ando, Y., Ando, E., Sun, X., Nakamura, M., Terazaki, H., Misumi, S., Tanoue, Y., Tajiri, T., Shoji, S., Ishizaki, T., Okabe, H., Tanihara, H., 2002. Presence of variant transthyretin in aqueous humor of a patient with familial amyloidotic polyneuropathy after liver transplantation. Amyloid 9, 247–251.

Herbert, J., Wilcox, J.N., Pham, K.T., Fremeau Jr., R.T., Zeviani, M., Dwork, A., Soprano, D.R., Makover, A., Goodman, D.S., Zimmerman, E.A., et al., 1986. Transthyretin: a choroid plexus-specific transport protein in human brain. The 1986 S. Weir Mitchell award. Neurology 36, 900–911.

Holmgren, G., Steen, L., Ekstedt, J., Groth, C.G., Ericzon, B.G., Eriksson, S., Andersen, O., Karlberg, I., Norden, G., Nakazato, M., et al., 1991. Biochemical effect of liver transplantation in two Swedish patients with familial amyloidotic polyneuropathy (FAP-met30). Clin. Genet. 40, 242–246.

Inada, K., 1988. Localization of prealbumin in human eye. Jpn. J. Ophthalmol. 32, 438–443.

Kanda, Y., Goodman, D.S., Canfield, R.E., Morgan, F.J., 1974. The amino acid sequence of human plasma prealbumin. J. Biol. Chem. 249, 6796–6805.

Kimura, A., Ando, E., Fukushima, M., Koga, T., Hirata, A., Arimura, K., Ando, Y., Negi, A., Tanihara, H., 2003. Secondary glaucoma in patients with familial amyloidotic polyneuropathy. Arch. Ophthalmol. 121, 351–356.

Martone, R.L., Schon, E.A., Goodman, D.S., Soprano, D.R., Herbert, J., 1988. Retinol-binding protein is synthesized in the mammalian eye. Biochem. Biophys. Res. Commun. 157, 1078–1084.

Munar-Ques, M., Salva-Ladaria, L., Mulet-Perera, P., Sole, M., Lopez-Andreu, F.R., Saraiva, M.J., 2000. Vitreous amyloidosis after liver transplantation in patients with familial amyloid polyneuropathy: ocular synthesis of mutant transthyretin. Amyloid 7, 266–269.

Ruiz-Moreno, J.M., Thillaye, B., de Kozak, Y., 1992. Retino-choroidal changes in endotoxin-induced uveitis in the rat. Ophthalmic Res. 24, 162–168.

Silva-Araujo, A.C., Tavares, M.A., Cotta, J.S., Castro-Correia, J.F., 1993. Aqueous outflow system in familial amyloidotic polyneuropathy portuguese type. Graefes Arch. Clin. Exp. Ophthalmol. 231, 131–135.

Soprano, D.R., Herbert, J., Soprano, K.J., Schon, E.A., Goodman, D.S., 1985. Demonstration of transthyretin mRNA in the brain and other extrahepatic tissues in the rat. J. Biol. Chem. 260, 11793–11798.

Soprano, D.R., Soprano, K.J., Goodman, D.S., 1986. Retinol-binding protein and transthyretin mRNA levels in visceral yolk sac and liver during fetal development in the rat. Proc. Natl Acad. Sci. USA 83, 7330–7334.

Tani, Y., 1999. PCR in situ amplification and catalyzed signal amplification: approaches of higher sensitive, non-radioactive in situ hybridization. Acta Histochem. Cytochem. 32, 261–270.

van Jaarsveld, P.P., Edelhoch, H., Goodman, D.S., Robbins, J., 1973. The interaction of human plasma retinol-binding protein and prealbumin. J. Biol. Chem. 248, 4698–4705.

Case II-2 of family 2 was a 90-year-old woman whose mother, children, and grandchildren were symptomatic patients with RP. She had no disturbance of night vision. Unfortunately, she could not visit our clinic to have a detailed assessment of her eyes.

The mutant mRNA was not expressed in the peripheral blood lymphocytes of Cases II-3, III-2, III-4, and III-5 in family 1. This finding suggested that the mutation induces functional loss of one allele resulting in haploinsufficiency.

The incomplete penetrance in RP11 could be attributable to the co-inheritance of a *PRPF31* gene defect and a low-expression of the wild-type allele.[6] Because a Chinese pedigree showed a high penetrance and a British family presented many asymptomatic carriers,[6,7] the expression of the wild-type allele of *PRPF31* gene may depend on the genetic background. To determine what genetic factors modulate the differential expression of the wild-type allele would be useful in the prognosis of family members with mutations.

In conclusion, we have identified two novel and one known mutations in three unrelated Japanese families with ADRP. This constitutes approximately 3% of the ADRP patients screened. There were also asymptomatic carriers in the Japanese population.

REFERENCES

1. Vithana EN, Abu-Safieh L, Allen MJ, et al. A human homolog of yeast pre-mRNA splicing gene, PRP31, underlies autosomal dominant retinitis pigmentosa on chromosome 19q13.4 (RP11). Mol Cell 2001;8:375–381.
2. Makarova OV, Makarova EM, Liu S, Vornlocher HP, Luhrmann R. Protein 61K, encoded by a gene (PRPF31) linked to autosomal dominant retinitis pigmentosa, is required for U4/U6+U5 tri-snRNP formation and pre-mRNA splicing. EMBO J 2002;21:1148–1157.
3. Kawamura M, Wada Y, Noda Y, et al. Novel 2336–2337delCT mutation in RP1 gene in a Japanese family with autosomal dominant retinitis pigmentosa. Am J Ophthalmol 2004;137:1137–1139.
4. Wada Y, Abe T, Takeshita T, Sato H, Yanashima K, Tamai M. Mutation of human retinal fascin gene (FSCN2) causes autosomal dominant retinitis pigmentosa. Invest Ophthalmol Vis Sci 2001;42:2395–2400.
5. Wada Y, Itabashi T, Sato H, Tamai M. Clinical features of a Japanese family with autosomal dominant retinitis pigmentosa associated with a Thr494Met mutation in the HPRP3 gene. Graefes Arch Clin Exp Ophthalmol 2004;242:956–961.
6. Vithana EN, Abu-Safieh L, Pelosini L, et al. Expression of PRPF31 mRNA in patients with autosomal dominant retinitis pigmentosa: a molecular clue for incomplete penetrance? Invest Ophthalmol Vis Sci 2003;44:4204–4209.
7. Wang L, Ribaudo M, Zhao K, et al. Novel deletion in the pre-mRNA splicing gene PRPF31 causes autosomal dominant retinitis pigmentosa in a large Chinese family. Am J Med Genet 2003;121:235–239.

Trans-Tenon Retrobulbar Triamcinolone Injection for Macular Edema Associated With Branch Retinal Vein Occlusion Remaining After Vitrectomy

Takahiro Kawaji, MD, Akira Hirata, MD, PhD, Nanako Awai, MD, Akiomi Takano, MD, Yasuya Inomata, MD, Mikiko Fukushima, MD, PhD, and Hidenobu Tanihara, MD, PhD

PURPOSE: To evaluate the effectiveness and safety of trans-Tenon retrobulbar triamcinolone injection for macular edema associated with branch retinal vein occlusion (BRVO) after vitrectomy.

DESIGN: Prospective interventional case series.

METHODS: The study included 20 eyes of 20 patients with BRVO, characterized by macular edema lasting more than 3 months after vitrectomy. Trans-Tenon retrobulbar injection of 40 mg triamcinolone was performed, and visual and anatomic responses were evaluated.

RESULTS: Mean foveal thickness was 499.4 ± 209.1 μm preoperatively, 281.8 ± 110.1 μm at 2-week follow-up, and 196.9 ± 92.1 μm at 6-month follow-up ($P < .0001$, at 2 weeks and 6 months, paired t test). Improvement of visual acuity by at least 0.2 logMAR (logarithm of the minimum angle of resolution) was seen in 14 (70%) of the 20 eyes.

CONCLUSIONS: Trans-Tenon retrobulbar injection of triamcinolone may be an alternative for additional treatment of eyes with BRVO that remains after vitrectomy.

RECENT INVESTIGATIONS HAVE DEMONSTRATED THE effectiveness of vitrectomy and its associated procedures for the decrease of macular edema in eyes with branch retinal vein occlusion (BRVO).[1] However, some cases of macular edema are resistant to vitrectomy. We evaluated the efficacy and safety of trans-Tenon retrobulbar triamcinolone injection for prolonged macular edema after vitrectomy in patients with BRVO.

Included in our study were 20 consecutive eyes of 20 patients with prolonged macular edema associated with BRVO lasting more than 3 months after vitrectomy.

Accepted for publication Feb 25, 2005.

From the Department of Ophthalmology and Visual Science, Graduate School of Medical Sciences, Kumamoto University, Kumamoto, Japan.

This study was supported in part by a Grant-in-Aid for Scientific Research from the Ministry of Education, Science, Sports and Culture, Japan, from the Ministry of Health and Welfare, Japan.

Inquiries to Hidenobu Tanihara, MD, PhD, Department of Ophthalmology and Visual Science, Graduate School of Medical Sciences, Kumamoto University, 1-1-1 Honjo, Kumamoto 860-8556, Japan; fax: (+81) 96-373-5249; e-mail: tanihara@pearl.ocn.ne.jp

TABLE 1. Baseline and Follow-up Data for 20 Patients Treated With Trans-Tenon Retrobulbar Triamcinolone Injection

Patient	Age (years)	Sex	Duration* (months)	Operation	Duration† (months)	Pre-VA	Final VA	Follow-up (months)	Recurrence
1	54	M	3	PEA + IOL + Vit (PVD)	10	0.1	0.4	14	+
2	68	M	26	PEA + IOL + Vit	9	0.08	0.04	14	−
3	78	F	3	PEA + IOL + Vit (PVD)	9	0.2	0.4	14	−
4	52	M	10	PEA + IOL + Vit (PVD)	7	0.1	0.3	13	−
5	50	F	1	Vit (PVD)	4	0.2	0.4	13	−
6	60	M	4	PEA + IOL + Vit (PVD)	21	0.2	0.5	13	−
7	84	F	3	Vit (PVD)	13	0.1	0.1	13	−
8	72	F	3	PEA + IOL + Vit (PVD)	3	0.2	0.4	13	−
9	69	M	2	Vit (PVD)	7	0.3	0.6	13	−
10	74	F	8	PEA + IOL + Vit (PVD)	13	0.1	0.3	12	−
11	73	M	26	PEA + IOL + Vit (PVD)	6	0.15	0.3	10	−
12	62	F	3	PEA + IOL + Vit	3	0.5	1	10	−
13	65	M	3	Vit (PVD)	4	0.3	0.4	7	−
14	67	F	4	PEA + IOL + vit (PVD, sheathotomy)	4	0.3	0.4	7	−
15	58	F	14	PEA + IOL + Vit (PVD, ILM)	10	0.3	0.6	6	−
16	79	F	2	PEA + IOL + Vit (PVD)	10	0.2	0.2	6	−
17	58	F	3	PEA + IOL + Vit (PVD, ILM)	3	0.3	0.4	10	−
18	61	M	9	PEA + IOL + Vit (PVD)	4	0.4	0.2	9	+
19	52	M	3	Vit (PVD)	5	0.1	0.2	8	−
20	59	F	7	PEA + IOL + Vit (PVD)	8	0.2	0.5	9	−

ILM = Peeling of the internal limiting membrane; IOL = intraocular lens implantation; PEA = phacoemulsification; PVD = surgical posterior vitreous detachment; VA = visual acuity; Vit = vitrectomy.

*Duration from onset of visual impairment to vitrectomy.

†Duration from vitrectomy to triamcinolone infusion.

Inclusion criteria were decimal best-corrected visual acuity of 0.5 or worse and foveal thickness greater than 250 μm. Trans-Tenon retrobulbar triamcinolone injection was performed as described previously.[2] Briefly, after topical anesthesia was administered, the conjunctiva and Tenon capsule were incised in the inferotemporal quadrant. A 23-gauge curved blunt cannula was then inserted into the sub-Tenon space, and 40 mg of triamcinolone acetonide was injected. Levofloxacin 0.5% was instilled four times daily for 1 week.

Data for all eyes are listed in Table 1. Mean ± SD duration between surgeries and triamcinolone injection was 7.7 ± 4.5 months (range 3 to 21). Mean follow-up period after injection was 10.7 ± 2.8 months (range 6 to 14). Mean foveal thickness was 499.4 ± 209.1 μm preoperatively, 281.8 ± 110.1 μm at 2-week follow-up, and 196.9 ± 92.1 μm at 6-month follow-up. Statistical analysis showed significant differences between preoperative and postoperative measurements ($P < .0001$ at 2 weeks and 6 months, paired t test). Visual acuity improved significantly from preoperative 0.74 ± 0.26 logMAR (logarithm of the minimum angle of resolution; range 1.1 to 0.3) to 0.46 ± 0.31 logMAR (range 1.0 to 0; $P < .0001$) at 6-month follow-up. Improvement of visual acuity by at least 0.20 logMAR was seen in 14 (70%) of 20 eyes. There were no eyes with visual loss of 0.20 logMAR or greater after injection. Fluorescein leakage area at late phase had decreased significantly at 1-month follow-up ($P = .0003$) from 10.5 ± 3.8 mm^2 (range 5.6 to 15.5) to 4.6 ± 2.6 mm^2 (range 2.6 to 7.7). Fluorescein leakage, which was evaluated subjectively in a masked fashion, in all eyes was improved. In two eyes, an additional injection was performed 3 and 6 months after the first because of recurrent macular edema. Intraocular pressure (IOP) elevation of 22 mm Hg or higher was found in seven (35%) of 20 eyes. IOP was controlled with antiglaucoma medications in all cases (Table 2). Cataract progression was noted in one of five phakic eyes.

Among the sequels to BRVO, macular edema directly affects the fovea and reduces visual acuity. Although vitreous surgeries are regarded as surgical modality for the treatment of macular edema, cases of macular edema do not always show anatomical or functional improvement in retinas after surgery. Recent clinical studies have shown that intravitreal injections of triamcinolone acetonide is effective for the treatment of macular edema.[3,4] However, intravitreal techniques carry the potential risks of vitreous hemorrhage, retinal detachment, and endophthalmitis,[5] as well as IOP elevation. Our results imply that in eyes even after vitrectomy,

TABLE 2. Summary of Changes in Foveal Thickness, Visual Acuity, and Intraocular Pressure*

Time Point	Foveal Thickness		logMAR Visual Acuity		IOP	
	Mean ± SD (μm)	*P* Value	Mean ± SD	*P* Value	Mean ± SD (mm Hg)	*P* Value
Baseline (n = 20)	499.4 ± 209.1	NA	0.74 ± 0.26	NA	12.2 ± 2.5	NA
2 weeks (n = 20)	263.5 ± 116.4	<.0001	0.49 ± 0.26	.0007	15.0 ± 4.2	.0004
1 month (n = 20)	231.8 ± 107.0	<.0001	0.48 ± 0.26	<.0001	15.8 ± 4.9	.0004
3 months (n = 20)	186.8 ± 67.7	<.0001	0.47 ± 0.28	<.0001	17.2 ± 7.1	.0018
6 months (n = 20)	192.5 ± 85.4	<.0001	0.46 ± 0.31	<.0001	15.1 ± 4.2	.0012
12 months (n = 10)	196.9 ± 92.1	.0116	0.51 ± 0.32	.0012	13.6 ± 3.0	.0772

IOP = Intraocular pressure; NA = not applicable.
*Differences were analyzed by the paired *t* test and considered significant when $P < .001$.

trans-Tenon retrobulbar injection of triamcinolone may be an alternative for additional treatment.

REFERENCES

1. Saika S, Tanaka T, Miyamoto T, Ohnishi Y. Surgical posterior vitreous detachment combined with gas/air tamponade for treating macular edema associated with branch retinal vein occlusion: retinal tomography and visual outcome. Graefes Arch Clin Exp Ophthalmol 2001;239:729–732.
2. Okada AA, Wakabayashi T, Morimura Y, et al. Trans-Tenon's retrobulbar triamcinolone injection for the treatment of uveitis. Br J Ophthalmol 2003;87:968–971.
3. Jonas JB, Sofker A. Intraocular injection of crystalline cortisone as adjunctive treatment of diabetic macular edema. Am J Ophthalmol 2001;132:425–427.
4. Gillies MC, Simpson JM, Billson FA, et al. Safety of an intravitreal injection of triamcinolone: results from a randomized clinical trial. Arch Ophthalmol 2004;122:336–340.
5. Moshfeghi DM, Kaiser PK, Scott IU, et al. Acute endophthalmitis following intravitreal triamcinolone acetonide injection. Am J Ophthalmol 2003;136:791–796.

Medial Canthal Tophus Associated With Gout

Yen Chang Chu, MD, Yi Yueh Hsieh, MD, and Lih Ma, MD

PURPOSE: To report a case with a gouty tophus at the medial canthus.

DESIGN: Observational case report.

METHODS: Review of the clinical, laboratory, photographic, and pathologic records of a patient with a gouty tophus at the medial canthus.

RESULTS: A 27-year-old man had a 3-year history of gouty arthritis and poorly controlled hyperuricemia. A medial canthal mass without discomfort developed gradually over 3 months. An excisional biopsy was performed, and the tissue was fixed in formalin for pathology. Analysis of a routine hematoxylin-and-eosin–stained section disclosed a multilobulated pseudocyst filled with amorphous eosinophilic material. Further staining with nonaqueous alcoholic eosin and viewed under a polarizing microscope indicated the presence of birefringent urate crystals.

CONCLUSIONS: Gouty tophus can develop progressively at the medial canthus, especially in people with uncontrolled hyperuricemia. A formalin-fixed specimen, stained with nonaqueous alcoholic eosin, demonstrates abundant birefringent urate crystals under a polarizing microscope. (Am J Ophthalmol 2005;140:542–544.

GOUT IS A COMMON RESULT OF VARIOUS DISORDERS that produce hyperuricemia. Deposition of urates in the joints may lead to recurrent attacks of arthritis. Tophi represent large aggregates of urate crystals and lead to inflammatory reactions. They are commonly seen in peripheral parts of the body but are rarely encountered by an ophthalmologist. We present a case with primary tophus formation at the medial canthus, which has not been reported in the literature.

A 27-year-old man came to our clinic for evaluation of a medial canthal mass in the right eye (Figure 1). The mass developed gradually over 3 months without discomfort. The patient denied previous trauma but had been diagnosed with gouty arthritis 3 years earlier. The arthritis involved only the proximal first metatarsal joint of the left foot. Because of recurrent attacks, the joint was mildly deformed. The patient did not control hyperuricemia regularly and only took medication during acute attacks. The concentration of serum uric acid was 10.4 mg/dl (normal range 3.8 to 7.0 mg/dL). Family history of hyperuricemia, but without gouty arthritis, was present in his mother and brother.

Accepted for publication Feb 25, 2005.

From the Departments of Ophthalmology (Y.C.C., L.M.) and Pathology (Y.Y.H.), Chang Gung Memorial Hospital, Taoyuan, Taiwan.

Inquiries to Lih Ma, MD, Department of Ophthalmology, Chang Gung Memorial Hospital, No. 5, Fu-Hsin Street, Kwei-Shan Shiang, Taoyuan, Taiwan; e-mail: malih1@adm.cgmh.org.tw

Available online at www.sciencedirect.com
SCIENCE DIRECT
Experimental Eye Research 82 (2006) 362–370
EXPERIMENTAL EYE RESEARCH
www.elsevier.com/locate/yexer

Rho-associated protein kinase inhibitor, Y-27632, induces alterations in adhesion, contraction and motility in cultured human trabecular meshwork cells

Tomoyo Koga[a], Takahisa Koga[a], Maiko Awai[a], Jun-ichiro Tsutsui[a], Beatrice Y.J.T. Yue[b], Hidenobu Tanihara[a,*]

[a]*Department of Ophthalmology & Visual Science, Kumamoto University Graduate School of Medical Sciences, Honjo 1-1-1, Kumamoto 860-8556, Japan*
[b]*Department of Ophthalmology and Visual Sciences, University of Illinois at Chicago, College of Medicine, USA*

Received 28 March 2005; accepted in revised form 11 July 2005
Available online 25 August 2005

Abstract

We investigated the roles of Rho-associated protein kinase (ROCK) in regulating activities such as adhesion, contraction and migration in cultured human trabecular meshwork (TM) cells. Human TM cells in culture were treated with Y-27632, a specific ROCK inhibitor. Trypan blue exclusion test and TUNEL staining showed little or no direct toxicity of Y-27632 on TM cells. By MTT assay, Y-27632 did not significantly affect the proliferation of TM cells. The cell adhesion assay showed that Y-27632 promoted the cell adhesiveness to both fibronectin and collagen type I in a dose-dependent manner. Collagen gel contraction activity of TM cells was significantly inhibited by the treatment of Y-27632 in a dose-dependent manner. The addition of Y-27632 accelerated motility of TM cells in wound healing assay. Phosphorylated LIM kinase 2 and cofilin, related to actin bundling and integrin clustering, were dephosphorylated (activated) by Y-27632. In conclusion, Y-27632 elicits profound effects on TM cell activities including adhesion, gel contraction, and cell motility. These Y-27632-induced changes of TM cells may be relevance to the physiology of the aqueous outflow system.

Keywords: Rho; ROCK; Y-27632; trabecular meshwork cells

1. Introduction

In human eyes, a majority (83–96%) of the aqueous humour leaves the eye through the trabecular meshwork (TM) and Schlemm's canal (conventional outflow) under physiologic conditions (Jocson and Sears, 1971; Bill and Phillips, 1971). Accumulating data have suggested that TM cells and their extracellular matrix (ECM) play important roles in regulating the conventional outflow pathway and the intraocular pressure (IOP). For instance, with aging, the aqueous outflow resistance increases while the number of TM cells decreases and the ECM composition in the juxtacanalicular region changes (Alvarado et al., 1981; McMenamin et al., 1986; Miyazaki et al., 1987). Fewer TM cells and abnormal deposition of the ECM have also been reported in glaucomatous eyes compared with normal eyes (Rohen, 1983; Alvarado et al., 1984; Alvarado et al., 1986; Knepper et al., 1996). It is believed that the outflow facility can be improved by modulating the TM cellular behaviour and that new IOP-lowering drugs may be designed through this process. So far, it has been reported that IOP can be reduced by cytoskeletal drugs such as cytochalasins (Kaufman and Barany, 1977; Kaufman and Erickson, 1982), ethacrynic acid (Epstein et al., 1987), a serine-threonine kinase inhibitor H-7 (Tian et al., 1998; Epstein et al., 1999), and protein kinase C inhibitor (Khurana et al., 2003).

Rho guanosine triphosphatase (GTPase), a member of the Rho subgroups of the Ras superfamily, participates in signalling pathways that play key roles in formation of actin stress fibres and focal adhesions, cytoskeletal rearrangements, cell morphology, cell motility and smooth muscle

Abbreviations effects of Y-27632 on human trabecular meshwork cells.

* Corresponding author. Hidenobu Tanihara, Department of Ophthalmology & Visual Science, Kumamoto University Graduate School of Medical Sciences, Honjo 1-1-1, Kumamoto 860-8556, Japan
E-mail address: tanihara@pearl.ocn.ne.jp (H. Tanihara).

0014-4835/$ - see front matter © 2005 Elsevier Ltd. All rights reserved.
doi:10.1016/j.exer.2005.07.006

contraction (Takai et al., 1995; Nobes and Hall, 1995; Kaibuchi et al., 1999). Recently, several putative target molecules of Rho have been identified as Rho effectors, including Rho-associated coiled coil-forming protein kinase named ROCK I (Nakagawa et al., 1996) (also known as p160 ROCK (Ishizaki et al., 1996)), and its isoform, ROCK II (Nakagawa et al., 1996) (also known as Rho kinase (Matsui et al., 1996) and ROK α (Leung et al., 1995)). ROCKs are important factors regulating focal adhesions and stress fibre formation in cultured fibroblasts and epithelial cells (Riento and Ridley, 2003). Y-27632 has been identified as a specific inhibitor of the ROCK/ROK family of protein kinases (Uehata et al., 1997). In a previous report from our laboratory, we noted that administration of this compound resulted in a significant reduction of IOP in rabbits in a dose-dependent manner (Honjo et al., 2001). We also demonstrated the presence of p160 ROCK in human TM cells and showed that ROCK inhibitors altered cell shape, disrupted actin bundles, and impaired focal adhesion formation (Honjo et al., 2001). Our studies along with others suggested that alterations in TM cellular behaviours might be the basis for the observed changes in the outflow facility (Tian et al., 2000; Lutjen-Drecoll et al., 2001; Rao et al., 2001).

Herein, we extended our effort in elucidating the physiology of the aqueous humour outflow by examining further the effects of Y-27632 on activities, including viability, proliferation, adhesion on the ECM, collagen gel contraction and motility of human TM cells in culture.

2. Materials and methods

2.1. Culture of human TM cells

Human eyes from donors aged 15, 22 and 47 years were obtained from the Illinois Eye Bank (Chicago). The procurement of tissues was approved by the Institutional Review Board at the University of Illinois at Chicago in compliance with the declaration of Helsinki. Trabecular tissues excised from eyes were cultured on Falcon Primaria flasks (Becton Dickson, Lincoln Park, NJ), as previously described (Yue et al., 1990; Sawaguchi et al., 1992; Zhou et al., 1996; Choi et al., 2005). The culture medium included Dulbecco's modified Eagle's medium (DMEM), 10% fetal bovine serum (FBS), and antibiotics. Cells were maintained at 37 °C in a 95% air −5% CO_2 incubator, and passaged using the trypsin-EDTA method. Human TM cells from passages 3 through 8 were used for subsequent studies.

2.2. Trypan blue exclusion test

The cytotoxicity of Y-27632 was evaluated using the trypan blue exclusion test. Viable cells were counted in vitro according to a previously described method (Jain et al., 1992). Briefly, 5×10^5 human TM cells were plated onto 100-mm dishes and grown for 24 hr. The medium was then replaced with fresh medium without or with Y-27632 (1, 10 and 100 μM). Twenty-four hour after the treatment, the cells were trypsinized and 1 mL of cell suspension containing 2×10^6 TM cells was prepared; 50 μL of 0.1% (vol/vol) trypan blue solution was then added to the cell suspension. Stained and unstained cells were counted by hemacytometer under a microscope 3 min after trypan blue treatment. The percentage of cell viability was calculated using the following formula: % cell viability=(viable cell count/total cell count)×100. Five independent experiments were performed.

2.3. Terminal deoxyribonucleotidyl transferase (TdT)-mediated fluroscein-16-dUTP nick end-labelling (TUNEL) assay

Human TM cells plated on glass coverslips in 12-well culture plates were grown at 37 °C for 24 hr. Y-27632 (10 and 100 μM) was added and incubated for an additional 24 hr. The cells were then fixed with 4% paraformaldehyde in phosphate-buffered saline (PBS) for 15 min, washed with PBS, and permeabilized with 0.2% Triton X-100 for 5 min. For positive controls, the cells were incubated with 1 unit mL^{-1} DNase I (Invitrogen, Carlsbad, CA) for 10 min. TUNEL reaction was performed with Apoptosis Detection System, Fluorescein (Promega, Madison, WI) at 37 °C for 60 min according to the manufacture's protocol. After mounting using an anti-fade kit (Molecular Probes, Eugene, OR), the staining was observed under a fluorescence microscope (IX71, Olympus, Tokyo, Japan).

2.4. Cell proliferation assay

Proliferation of cultured human TM cells was measured by 3, (4,5-dimethyl-2-thiazolyl)-2,5-diphenylate-2Htetrazolium bromide (MTT), using a commercially available kit (Nacalai Tesque, Kyoto, Japan). Cells were plated in culture medium at a density of 1×10^4 cells per well in 96-well plates and allowed to adhere for 24 hr. After washing, the cultures were fed with fresh media, without or with Y-27632 (1, 10 and 100 μM) for 72 hr, and finally treated with 5 mg mL^{-1} MTT for 4 hr at 37 °C. The MTT solution was aspirated, and the formazan crystals were dissolved in detergent reagent for 10 min. The relative cell number was determined based on the optical absorbance of the formazan at 570 nm, using a control wavelength of 655 nm measured in automatic plate reader (BioRad, Hercules, CA).

2.5. Cell adhesion assay

Cell adhesion assay was conducted as previously described (Zhou et al., 1996). For the assay, the wells of 96-well plates were coated overnight with fibronectin (10 μg mL^{-1}) (Sigma, St. Louis, MO) or collagen type I (0.5 μg mL^{-1}) (Calbiochem, San Diego, CA) at 4 °C.

The remaining binding sites were blocked by 0.1% of bovine serum albumin (BSA) in PBS for 2 hr at room temperature. Human TM cells were suspended in culture medium containing 2 mg mL^{-1} of BSA without or with Y-27632 (at 10 or 100 μM), and were loaded ($n=4$) onto coated wells at 8×10^4 cells per well. After incubation for 60 min, the unattached cells were removed by aspiration. The remaining cells were fixed in 10% formalin and stained with 1% toluidine blue. They were then lysed and the intensity of the blue stain was measured with a microplate reader at 600 nm as an indication of cell density.

2.6. Immunocytochemical studies

TM cells were plated on glass coverslips in culture medium, and cultured overnight. Y-27632 at 100 μM was added for 60 min. After the drug exposure, the cells were fixed and permeabilized for 2 min in 3% paraformaldehyde-PBS with 5% Triton X-100 (Wako, Osaka, Japan), and were further fixed for 20 min with 3% paraformaldehyde. The samples were blocked in 2% BSA for 30 min. The coverslips were incubated for 60 min at room temperature with anti-β-catenin antibody (Sigma) diluted at 1:2000, or anti-pan-cadherin antibody (Abcam, Cambridgeshire, UK) diluted at 1:500 with blocking solutions. The samples were washed 3 times with PBS and incubated with Cy-3 conjugated anti-mouse secondary antibody (Jackson ImmunoResearch, West Grove, PA) or FITC conjugated anti-mouse secondary antibody (Jackson ImmunoResearch) for 30 min. After washing, the cells were mounted with anti-fade and observed by fluorescence microscope IX71.

2.7. Immunoblot analysis

Human TM cells (2×10^5 cells per well) were plated overnight in 6-well Falcon plates and were incubated with 10 or 100 μM of Y-27632 for 0.5 or 1 hr. Immediately after Y-27632 incubation or following a recovery period of 2 hr, the cells were gently washed with PBS and lysed in 500 μL of NuPAGE LDS sample buffer (Invitrogen) containing 0.05 M DTT (Invitrogen). The NuPAGE LDS sample buffer was commercially available, and consisted of 109 M Glycerol, 140.5 mM Tris, 106 mM Tris–HCl, 73 mM Lithium Dodesyl Sulfate, and 0.51 mM EDTA. After heating at 70 °C for 10 min in sample buffer, 15 μL of each sample was subjected to 4–12% NuPAGE Bis-Tris gel (Invitrogen) or 4–20% Tris-Glycine gel (Invitrogen) electrophoresis and transferred to nitrocellulose membrane (Protran, Schleicher and Schuell Bioscience, Keene, NH). The membrane was blocked for 60 min at room temperature in 5% skim milk and 0.1% Tween-20 diluted in Tris-buffered saline (TTBS) to minimize nonspecific immunoreaction. Some membranes were incubated for 1 hr at room temperature with anti-β-catenin antibody diluted at 1:4000, anti-pan-cadherin antibody diluted at 1:1000, anti-β-actin antibody (Ambion, Austin, TX) diluted at 1:500, or anti-glyceraldehyde 3-phosphate dehydrogenase (GAPDH) antibody (Biogenesis laboratories, Kommetjie, South Africa) diluted at 1:200 with dilution buffer (5% BSA in TTBS). Other membranes were subsequently incubated overnight at 4 °C with anti-phospho-LIM kinase 1/2 (Cell Signalling), anti-cofilin (Cell Signalling) or anti-phospho-cofilin (Cell Signalling) antibody diluted at 1:1000 with dilution buffer. The membrane was washed three times at room temperature for 10 min with TTBS. It was then incubated for 30 min at room temperature with horseradish-peroxidase-conjugated anti-mouse IgG antibody (1:500, Amersham Biosciences, Buckinghamshire, UK). After further washing, the membranes were incubated with enhanced chemiluminescence (Amersham Biosciences) and exposed to autoradiogram film to visualize immunoreactive bands.

2.8. Gel contraction assay

Collagen gel contraction assay was performed as previously described (Nakamura et al., 2002; Nakamura et al., 2003), with minor modifications. The wells of 24-well culture clusters were each coated at 37 °C with 1% BSA for 1 hr. Human TM cells were trypsinized and resuspended in culture medium at a density of 2.2×10^6 cells mL^{-1} without or with Y-27632 (1, 10 and 100 μM). Collagen type I (Nitta-gelatin, Osaka, Japan), 10×DMEM, reconstitution buffer (Nitta-gelatin), TM cell suspension and water were mixed in an ice bath at a ratio of 7:1:1:1:1 (final concentration of collagen type I, 1.9 mg mL^{-1}; final cell density, 2×10^5 cells mL^{-1}). The resultant mixture (0.5 mL) was added to each well of the BSA coated culture clusters, and collagen gel formation was induced by incubation at 37 °C for 90 min. DMEM (0.5 mL), without or with Y-27632 (1, 10 and 100 μM), was then added on top of the collagen gels. After 1 hr, the gels were freed from the walls of the culture wells with the use of a micro spatula. The diameter of the collagen gels was scanned into a computer and measured with a ruler every 24 hr for 3 days. The extent of contraction of the collagen gels mediated by the TM cells was expressed as decrease in gel diameter compared with the initial diameter.

2.9. Measurements of wound healing (cell motility) activities

Human TM cells were grown to confluence in 100-mm tissue culture dishes. Three or four sites in each dish were scraped from the confluent cells with a yellow plastic pipette tip to create a cleared line. The medium was removed and replaced with fresh medium without or with Y-27632 (10 and 100 μM). After incubation at 37 °C for 9 hr, the progress of cells moving into the wound area was photographed by microscope digital camera, DP70 (Olympus) and loaded into computer software, DP controller (Olympus). The shortest distance between the

edges of migrated TM cells (including its' protrusions) from both sides was measured by the ruler of this computer soft.

2.10. Stastical analysis

Data are presented as the mean ± S.D. and were statistically analysed by Student's *t*-test.

3. Results

3.1. Toxicologic experiments of Y-27632 on human TM cells

Trypan-blue exclusion test was performed to determine whether Y-27632 was toxic to TM cells. The percentage of the living TM cells without trypan blue staining was 99.7 ± 0.4% in control cultures without Y-27632 treatments ($n=5$). In experimental cultures treated with various concentrations of Y-27632, the percentages of trypan blue free (living) cells were between 99.4 and 99.6% ($n=5$), not statistically significant different from that in controls (Table 1). TUNEL staining was performed to investigate directly the effect on human TM cell death by the addition of Y27632. After treatments with DNase I, almost all of the TM cells became TUNEL-positive (Fig. 1). On the other hand, no TUNEL-positive cells could be detected even after 24 hr of Y-27632 treatment, although typical morphological changes were evident by light microscopy. Effects of Y-27632 on proliferation in cultured TM cells were evaluated with the use of MTT assay. No statistically significant differences between Y-27632 treated TM cells and controls could be discerned (Fig. 2). This inhibitor thus displayed little cytotoxicity and had no effect on the proliferative activity of TM cells.

3.2. Influence of Y-27632 on adhesion of TM cells onto ECM

To elucidate interactions between cultured human TM cells and ECM components, adhesion of TM cells onto

Table 1
Trypan blue exclusion test to evaluate cytotoxicity of Y27632 on cultured TM cells

	Exp. 1	Exp. 2	Exp. 3	Exp. 4	Exp. 5	Mean ± S.D.
TM (control)	100	100	100	99.2	99.3	99.7 ± 0.4
TM + Y27632 (1 μM)	98.9	99.1	100	100	99.4	99.4 ± 0.5
TM + Y27632 (10 μM)	100	99.1	100	100	98.9	99.6 ± 0.5
TM + Y27632 (100 μM)	99.1	100	100	99.1	100	99.6 ± 0.5

The percent of viable cells are shown. S.D., standard deviation; Exp, experiment.

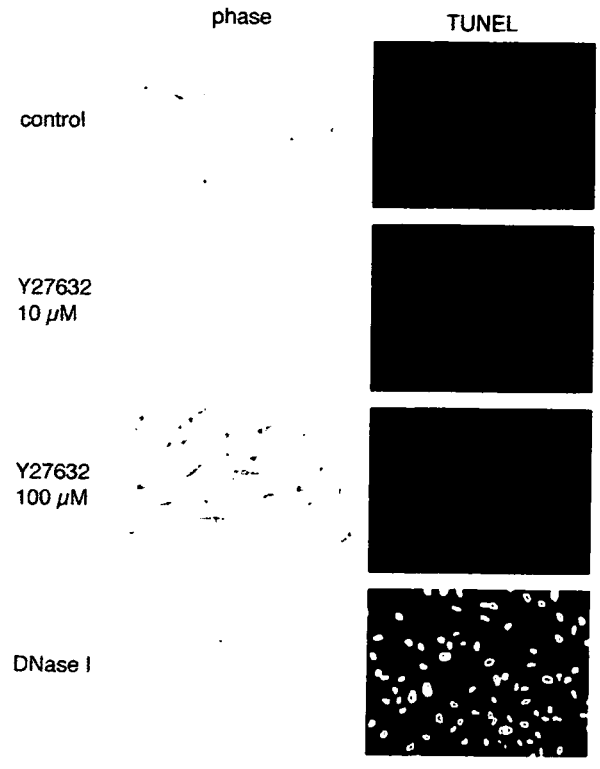

Fig. 1. Terminal deoxyribonucleotidyl transferase (TdT)- mediated fluroscein-16-dUTP nick end-labelling (TUNEL) staining on human TM cells without (control) or with the Y-27632 treatment for 24 hr. TUNEL positive cells were undetectable in TM cultures regardless whether they were untreated or treated with 10 μM or 100 μM Y-27632. In positive controls in which TM cultures were treated with DNase I, almost all of the cells were TUNEL positive (green).

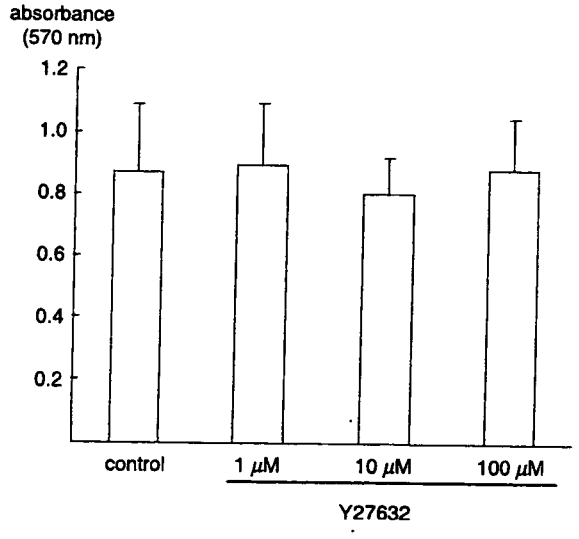

Fig. 2. Effect of Y-27632 on proliferation in human TM cells. Proliferation was measured by 3,(4,5-dimethyl-2-thiazolyl)-2,5-diphenylate-2H-tetrazolium bromide (MTT) assay. The data were expressed as the mean ± S.D. ($n=8$). Y-27632 did not affect human TM cell proliferation at any of concentrations (1, 10 or 100 μM).

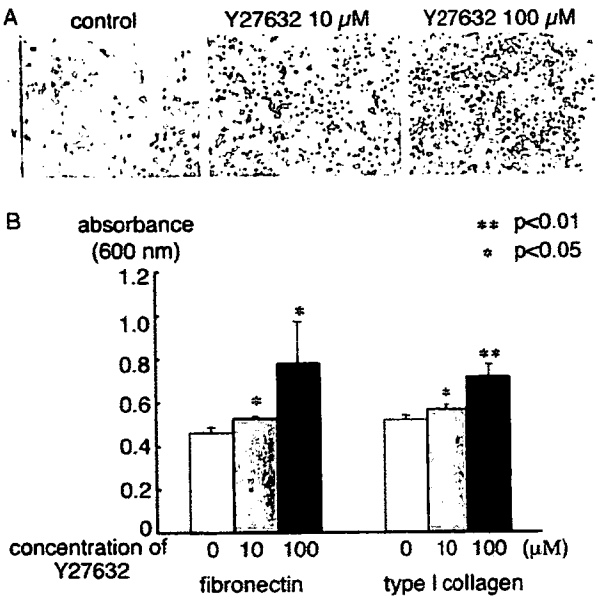

Fig. 3. Effect of Y-27632 on adhesion of human TM cells. Cells were plated on fibronectin (10 μg mL^{-1}) or collagen type I (0.5 μg mL^{-1}), and allowed to adhere in the absence or presence of Y-27632 (10 or 100 μM) for 60 min. The adhered cells were stained with 1% toluidine blue. The stained cells were lysed and the absorbance at 600 nm, a reflection of cell density, was measured. Data expressed as mean ± S.D. ($n=4$) were analysed by Student's t-test. The stained cells that were adhered on fibroectin are shown in A. Quantitative data are shown as bar graphs in B.

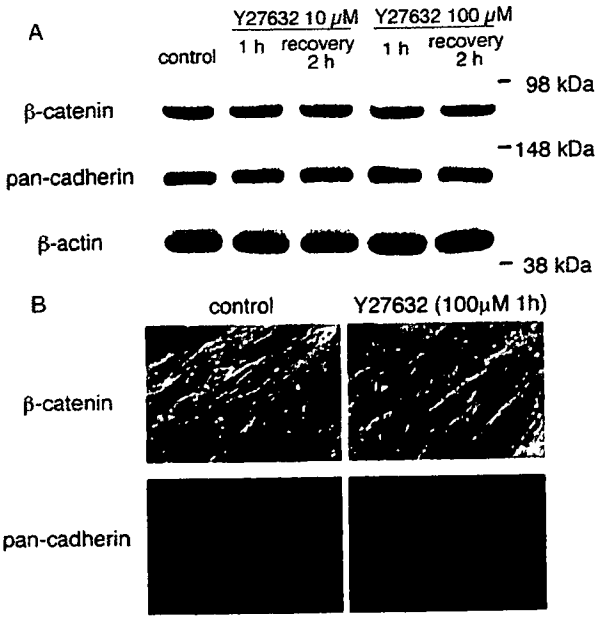

Fig. 4. (A) Level of β-catenin and pan-cadherin proteins in human TM cells treated with 0 (control), 10, or 100 μM of Y-27632. Immunoblot study was performed using lysates of cells collected immediately after Y-27632 treatment for 1 hr, or after incubation with fresh culture media without Y-27632 for an additional 2 hr (recovery 2 hr). (B) Distribution of β-catenin and pan-cadherin in human TM cells 1 hr after exposure to 100 μM of Y-27632. Experiments were repeated 3 times, yielding similar results.

fibronectin-coated or collagen type I-coated dishes was assayed. Compared with controls, a greater number of Y-27632-treated TM cells adhered onto fibronectin. Adhesion of TM cells to collagen type I was also increased by the addition of Y27632. The TM adhesion to both fibronectin and collagen type I was increased with increasing concentrations of Y-27632 (Fig. 3).

3.3. Effect of Y-27632 on cell–cell junction

In immunoblot analysis of cell–cell adhesion molecules, β-catenin (using anti-β-catenin antibody) and cadherins (using anti-pan-cadherin antibody) were detected under control medium without Y27632. These expression levels were not changed after Y27632 treatment for 1 hr and recovery for 2 hr. In immunocytochemical study, under control medium without Y27632, the cell–cell adhesions delineated by β-catenin and cadherins staining appeared as continuous or partially segmented lines along cell borders. After Y27632 treatment, these staining were also detected as continuous or partially segmented lines along borders of packed TM cells (Fig. 4).

3.4. Gel contraction assay

TM cells are known to induce contraction of collagen gel within which they are cultured (Nakamura et al., 2002; Nakamura et al., 2003). In our experiments, 24 hr after plating human TM cells with collagen gels, the change of the diameter of gels from the original value (16 mm) was 6.89 ± 0.38 mm ($n=3$). On the other hand, with 1, 10 and 100 μm Y-27632, the change of collagen gel diameter was 5.8 ± 0.8, 0.2 ± 0.4 and 0 mm (no detectable changes), respectively (Fig. 5). The results were statistically significant ($p<0.001$) and a dose dependency was evident. Similar results were also seen in experiments at 48 and 72 hr time points.

3.5. Wound healing (cell motility) activity of TM cells

Human TM cells in confluent cultures were scraped with a pipet tip to create cell-free wounds. At 9 hr after the scraping, the distance between the edges of exposed region was measured to be 75.0 ± 16.2, 28.1 ± 9.4 and 3.1 ± 5.4%, respectively, with Y-27632 at 0 (control), 10 and 100 μm (Fig. 6). The increase in the wound healing (cell motility) activity by Y-27632 was significant and concentration dependent.

In an effort to elucidate mechanisms related to actin remodelling and migration activities, we studied the status of phosphorylated forms of LIM kinase and cofilin. It has been reported that dephosphorylated LIM kinase leads to the dephosphorylated (active) form of cofilin, resulting in depolymerization of actin filament and promoting actin remodelling (Bamburg, 1999). Our immunoblot analysis showed that Y-27632 decreased the level of both